University of Stavanger

Faculty of Science and Technology

MASTER'S THESIS

Study program / Specialization: Petroleum Engineering / Reservoir Engineering	Spring semester, 2010 OPEN
Writer: Miftachul Choiri	..... (Writer's signature)
Faculty supervisor (s): Prof. Aly A. Hamouda External supervisor(s):	
Title of thesis: Study of CO_2 Effect on Asphaltene Precipitation and Compositional Simulation of Asphaltenic Oil Reservoir	
Credits : 30 ECTS	
Keywords: Asphaltene, resin, precipitation, deposition, compositional simulation, Flory-Huggins polymer-solution theory, Hildebrand, solubility parameter, CO2 flooding.	Pages: 70 + Enclosure: 35 Stavanger, 30th June , 2010

ABSTRACT

A model which is based on Flory-Huggins polymer-solution theory and Hildebrand solubility concept has been developed which shows an excellent match with experimental data. The fine-tuned model is then possible to predict weight percent of precipitated asphaltene at wide range of conditions (changes in pressure, temperature and composition). The prediction can be used to identify at which conditions lead to precipitation of asphaltene.

The procedure of calculation is quite simple compared to any other models which involve many requirements of parameters which most of them are difficult to estimate (complicated).

A compositional simulation is performed using a simple reservoir model to study effect of dynamic conditions to asphaltene behavior. The main objective of simulation is to investigate temperature effect during CO_2 flooding. It has been reported that temperature can have reverse effect from the normal convention. Comparison performance between CO_2 and water flooding are also simulated.

Quantification of asphaltene deposition and permeability reduction are carried out to give a clear picture on “how much” asphaltene deposits and “when” deposition of asphaltene is more pronounced.

Keywords:

asphaltene, resin,precipitation, deposition, compositional simulation, Flory-Huggins polymer-solution theory, Hildebrand, solubility parameter, CO_2 flooding.

ACKNOWLEDGEMENTS

Firstly, I would like to express my sincere gratitude to Allah by saying "Alhamdulillah" for giving me a strong faith and wonderful moments in entire of my life. Everything I have achieved so far is a gift of Allah.

This thesis is the final requirement to complete my Master degree at Department of Petroleum Engineering, University of Stavanger, Norway.

I would like to take this opportunity to thank my supervisor, Professor Aly A. Hamouda for his support, constructive ideas and extensive discussions which enlightens me for being better person.

Enormous thanks to my families who always pray for their children even they are separated thousands of miles away from Norway.

I am especially grateful to my fiancé, Lely Triyana, who continuously encourages me to keep maintaining the fighting spirit and for her never-ending love, support and understanding during my study in Norway.

I also want to thank University of Stavanger for awarding me a scholarship for two-year study.

Last but not least, special appreciation to all Indonesian friends for being such best friends and parents for me during my stay in Norway. I really enjoyed every moments.

Much gratitude is dedicated to all people that I can not mention one by one those helped this thesis was completed and delivered in timely manner.

Stavanger, 30th June 2010

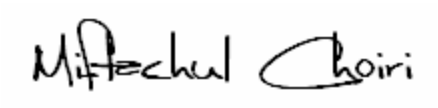

TABLE OF CONTENTS

LIST OF FIGURES

LIST OF TABLES

CHAPTER 1 INTRODUCTION

1.1 Background

A goal of petroleum industries is mainly focusing on enhancing the recovery factor as much as possible in accordance with cost effectiveness. During production whether in primary depletion or enhanced recovery phases, an operator attempts to maintain an optimum productivity and avoid potential production problems.

Changes of operating circumstances such as pressure, temperature and composition of the oil trigger production of heavy organic deposition, especially the presence of asphaltene deposits which have been reported as serious problems that cause severe losses in productivity of wells. There are many factors affecting asphaltene precipitation and deposition, Kokal and Sayegh[3] described which of those factors are important causing asphaltene precipitation in the reservoir and processing facilities.

Asphaltene is the heaviest component in crude oil. Initially, asphaltene is dissolved in crude oil. Once asphaltene is separated from the crude oil due to pressure loss or composition change in addition of solvents, asphaltene may deposit over surface rock and plug some pore throats that produce more flow resistance for oil in porous medium. Consequently, these depositions by time at certain concentration can induce significantly formation damage.

In recent years, most of oil reservoirs have reached economic limit of production by natural depletion and waterflooding. Applications of enhanced oil recovery (EOR) have been widely used to improve the oil recovery. One of popular EOR method is a miscible-CO2 flooding because CO2 is well-recognized more soluble in oil than water. Miscibility is achieved by eliminating the interfacial tension between oil and CO2. An injection of CO2 may contact with oil and cause changes in fluid behavior and equilibrium which is favorable condition for asphaltene to precipite. Therefore, precipitation of asphaltene is common in most CO2 flooding.

Mitigation of asphaltene deposition needs to be taken to eliminate massive additional costs: deposit removal treatments, loss of productivity because of shutdown and even loss of some wells (see

table 1.1). The likelihood of deposition problems is more prominent for exploitation of deep water operation.

Table 1. 1 Typical additional cost due to occurrence of asphaltene deposit problems[4]

Operation	Cost
Removal deposit	$300K- $3,500K/well
Side track	$50,000K/well
Downtime	$700K/day (for production of 7,000BPD)

It is fully understood that why many industries wish to have a predictive tool that allows them to design an efficient operation processes. By having a good knowledge of when and how much asphaltene precipitation and deposition, industries can avoid risks associated with asphaltene deposition problems and integrate this information to obtain better estimation of the economic field operation and development as result of the anticipated strategies.

Precipitation of asphaltene is a complex process and still not fully understood yet at the moment. Hence, there are various models had been reported in the literature for predicting the amount of asphaltene precipitation such as approaches which were based on the use of Flory-Huggins polymer solution theory[5, 6], application of equations of state computations[7, 8], utilization of thermodynamic colloidal models[9], and thermodynamic micellization models[10]. However, all techniques require an enormous experiment and time-consuming work to analyze the results. Most industries would like to have a practical tool which enables to estimate accurately the asphaltene precipitation, especially with respects to CO2 injection condition.

An attempt has been made to produce such tool to predict the asphaltene precipitation. That tool is believed to be able to calculate how much precipitated asphaltene will be produced at different pressure, temperature and composition of oil.

It has been observed that the proposed model is able to predict the weight percentage of asphatene precipitation using experimental data from different literatures in close agreement. The outcomes can be a map of asphaltene precipitation that is usually called as Asphaltene Deposition Envelope (ADE). This ADE is valuable for industries to determine at which condition an enormous deposition of asphaltene takes place.

Several papers reported that asphaltene precipitation is believed as a reversible process[11, 12]. Hence, a compositional simulation is performed to study the mechanisms of asphaltene deposition such as plugging, adsorption and entrainment.

In addition, CO_2 is well-known as the most effective method to achieve miscibility between oil and CO_2 by eliminating interfacial tension (IFT) and capillary forces to recover all residual oil[13]. On the contrary perspective, CO_2 also causes destabilization of asphaltene equilibrium because CO_2 results PH shifts[14] and changes oil composition. It is such a favorable conditions for asphaltene being deposited due to much exposure to a low PH environment (in general, PH is less than 4)[15].

As explained previously, ncluding a research on light hydrocarbon gases injection such as CO_2 with respects to asphaltene precipitation. In this work, the likelihood of asphaltene precipitation due to presence of CO_2 needs to be assessed. To do this assessment, a compositional simulation with CO_2 injection is initiated to run several possible scenarios and present which of parameters play an important role on asphaltene precipitation and deposition.

1.2 Objectives of the study

Generally, the studies mainly emphasize on the effect of pressure, temperature and composition changes on the asphaltene precipitation and deposition.

A composition of reservoir fluid system is quite important as pressure and temperature. Therefore, the compositional effects on properties of solution are addressed in the second part. The main task of present work is to improve a model that had been developed

by Hamouda et al[16]. The model used is a modification of Florry-Huggins polymer solution theory which relies on determination of solubility parameter of asphaltene-rich phase and asphaltene-free phase (liquid phase). (Enormous techniques have been published to calculate the solubility parameters for both phases. However, most of them are such equations of state which are not handy approaches can be used by industries.) An extensive effort has been made to test different approaches to determine and apply the solubility parameters to the available literature data. Hence, provide effective operating conditions.

The assumption of an irreversible process for asphaltene precipitation[17] has been taken for the studies mentioned above. It means that there is no entrainment process when asphaltene has been deposited and trapped on the rock reservoir. Attempted works to show and examine a reversibility of asphaltene deposition is accomplished using a commercial reservoir simulator (ECLIPSE™ in this study was used) to model asphaltene deposition and to demonstrate its impacts on reservoir.

A feature of asphaltene deposition modeling in a reservoir simulator ECLIPSE can only be performed in compositional simulation mode (E300). Many keywords are specified to make sensitivities analysis successful to deal with a wide range of governing variables related to asphaltene behavior in order to show the effects of those variables on recovery of oil as a result of asphaltene deposition.

1.3 Thesis contents

The main intention of thesis is to model asphaltene precipitation and validate the model with experimental results. The tuned model is then being able to predict the amount of precipitated asphaltene at a wide range of pressure, temperature and composition of oil due to CO_2 injection. All results are presented in 3-Dimensional graph. From such figure, it can be examined which factors are more pronounced to the asphaltene precipitation process.

A compositional simulation is initiated to address the sensitivity of the different asphaltene precipitation and deposition parameters with respect to oil recovery such as temperature, concentration of CO_2 in

oil, ratio of asphaltene over resin, adsorption, plugging, entrainment etc.

Chapter 2 presents literature review of asphaltene deposition problems to affect in production systems, mechanism of asphaltene precipitation, several pre-screening approaches to predict asphaltene precipitation which are commonly used by industries. In addition the established measurements of asphaltene precipitation in laboratory are discussed.

In Chapter 3, data and methodology are presented. All procedures are given in flowcharts for simplicity. Chapter 4 is a discussion of the results. Finally, chapter 5 includes the conclusion of this work. Appendix contains the computation, derivation and other data generated in this work.

CHAPTER 2 LITERATURE REVIEW

2.1 Flow Assurance Overview

Flow assurance has been a key topic of production issues in recent years as a rapid movement of production systems to deepwater environment (offshore operation)[18]. The term of flow assurance is very general used to evaluate the impact of processes that take place during production/injection. A hydrocarbon solid deposition (asphaltene in particular) can disrupt production in the flow system i.e. reservoir formation, wellbore and flowlines and separation facilities (as shown in Figure 2.1) is discussed.

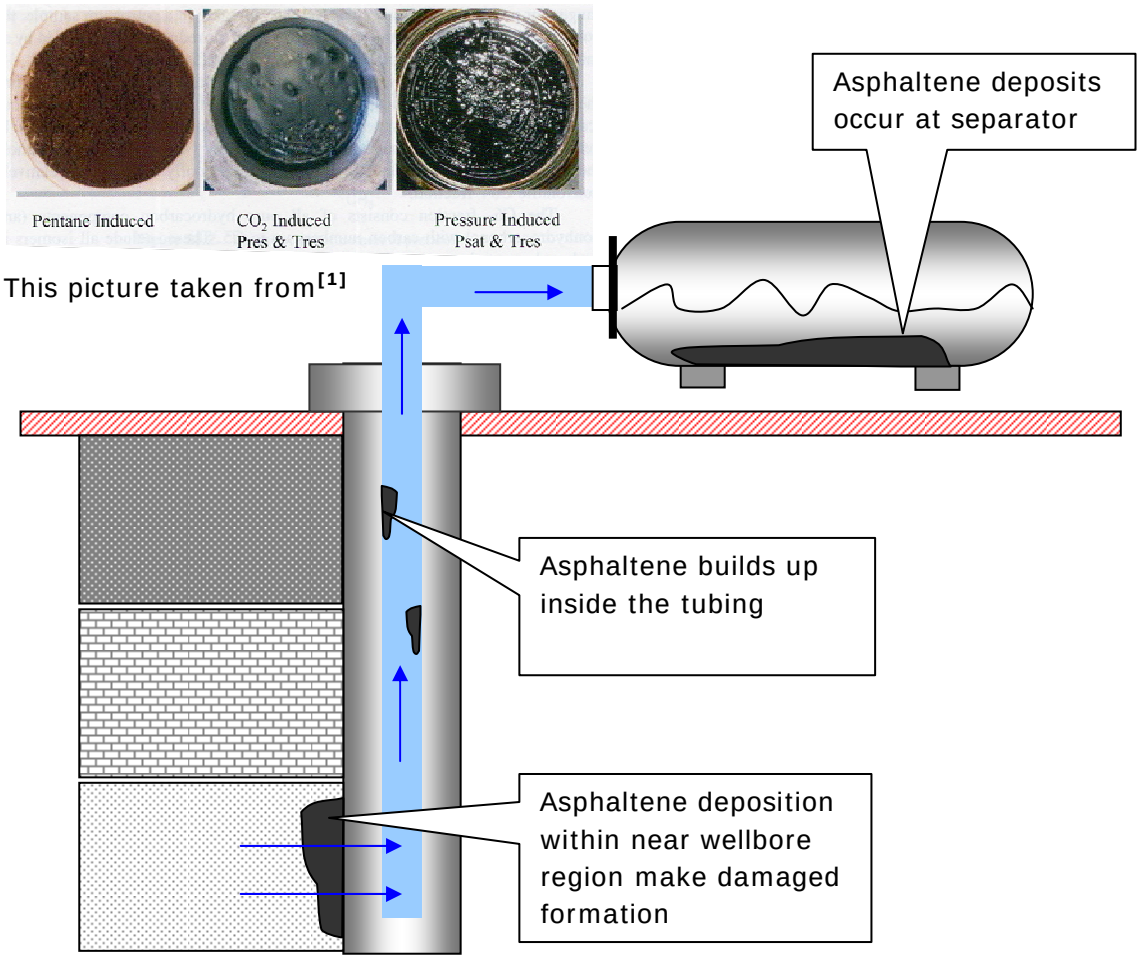

Figure 2.1 Asphaltenes Deposition in Flow Systems

In deep offshore field, the operation is more challenging than land-based fields because of dealing with extreme production conditions where temperature near freezing point and pressure drop from reservoir through facility are quite large. These extreme circumstances could lead to the precipitation and deposition of hydrocarbon solids i.e. waxes, asphaltenes and hydrates. Those precipitated solids are produced by different mechanisms. However, they are strongly influenced by Pressure and Temperature. As a rule of flow assurance framework, a solid precipitation behavior as a function of Pressure and Temperature are normally represented as solid boundary lines that are embedded on P-T diagram. The reason why those solid phase boundaries are plotted together is to seek at which Pressure and Temperature has solid free or likely less of solid production.

During production, fluid is moving from reservoir and wellbore, then transported through flowlines to separator. At that time, some solid phase boundaries are probably crossed as shown in Figure 2.2 resulting precipitation and deposition of solid than can have detrimental effect on economic of field operation.

As pressure decreases (in depleted phase), phase transition may occur and it could be quite problematic. If solid phases are formed, an unfavorable condition such as permeability reduction or blocking in production systems will lead to decrease the oil recovery and increase number of associated stimulation program to damaged wells, consequently, it results a significant operating cost.

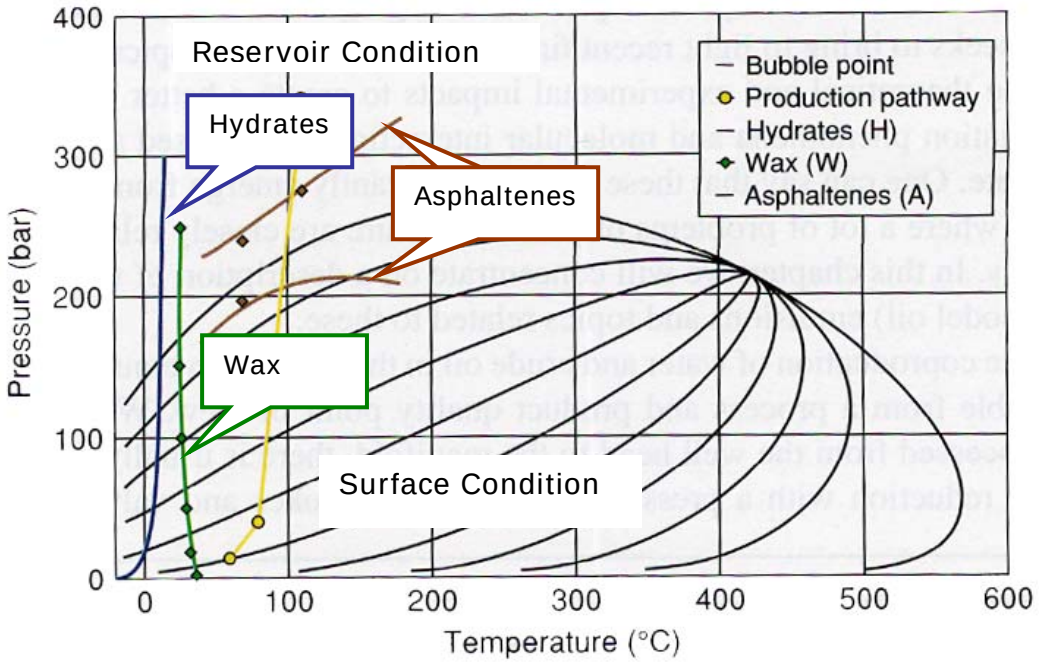

Figure 2.2 Schematic illustration of thermodynamic conditions of the flow assurance elements with boundaries of solids formation[1]

A better understanding of phase behavior is crucial due to highly potential to phase separate and aggregate with changes in temperature, pressure and composition of crude oil. A P-T diagram establishes a region where abundant precipitation of asphaltene formed which represents the limiting parameters (pressure, temperature and composition) that industries must avoid during production process to assure the process of oil recovery at a secured operation without precipitation of asphaltene.

2.2 Asphaltene Definition

Asphaltenes are high molecular weight (the heaviest fractions in crude oil) organic substances which soluble in aromatic solvents (e.g. toluene or benzene) but precipitated by addition of n-alkenes (e.g n-heptane or n-pentane). In other words, asphaltene is generally defined as n-pentane-insoluble and benzene-soluble fraction.

Crude oil is considered to be a colloidal system while asphaltenes are disperse phase. Asphaltene tends to remain in solution (colloidal suspension) stabilized and maintained by resins under reservoir pressure and temperature conditions[9, 11, 19, 20].

Asphaltenes carry an intrinsic charge of positive or negative depending on oil composition[14]. Resins have a strong tendency to associate with asphaltenes due to their opposite charge and are adsorbed by asphaltenes becomes a protective shield for asphaltenes[21]. When this protective shield of resins is removed, it might lead to the precipitation of asphaltenes. The destabilization of colloidal system is strongly influenced by force balance between adsorbed resin and asphaltene[22]. An illustration of the resin can be described in figure 2.3 showing force balance between the adsorbed resin molecules and asphaltenes particles where the polar heads of the resins are covering the asphaltenes.

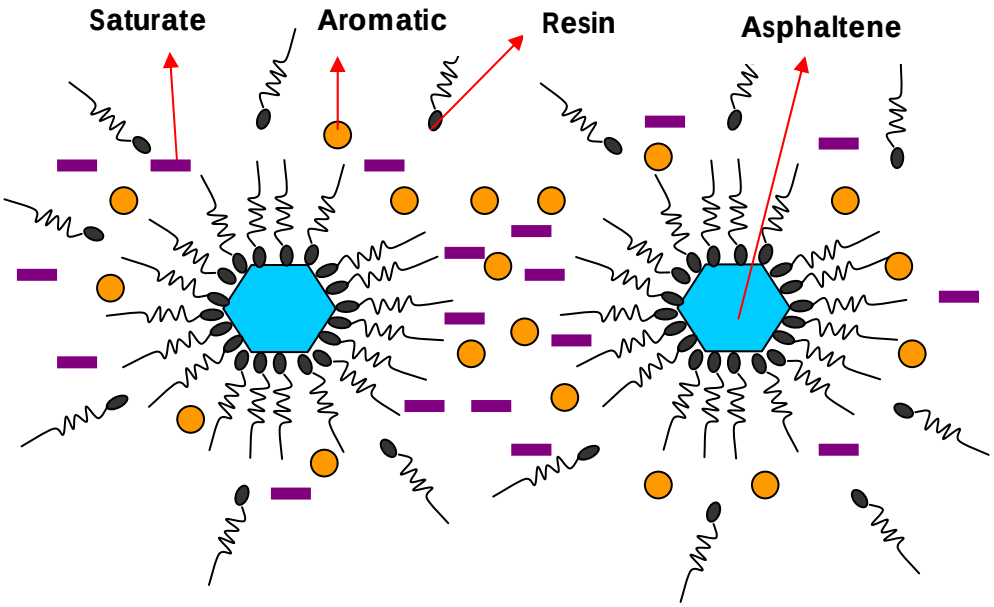

Figure 2.3 An illustration of force balance on asphaltenes[1]

As temperature or pressure changes, asphaltene may start to precipitate because of instability condition of colloidal suspension.

A simple way to determine the paraffinicity or aromaticity of crude oil is from the ratio of hydrogen to carbon atoms (H/C). As crude oil becomes more compact, more aromatic rings with less hydrogen, the H/C ratio becomes low. Normaly, H/C ratio of resins is from 1.3 to 1.6 and 1 to 1.3 for asphaltenes[15].

SARA (saturate, aromatic, resin and asphaltene) analysis is widely used to identify the fractions of crude oil that affect the asphaltene stability. The saturate fraction consists of nonpolar material and aromatic fraction is more polarizable. Both resin and asphaltene have polar constituents but the difference between them depends on miscibility with n-pentane or n-heptane, asphaltene is insoluble, while resin is miscible[15]. The SARA fractions are described and summarized in Figure 2.4.

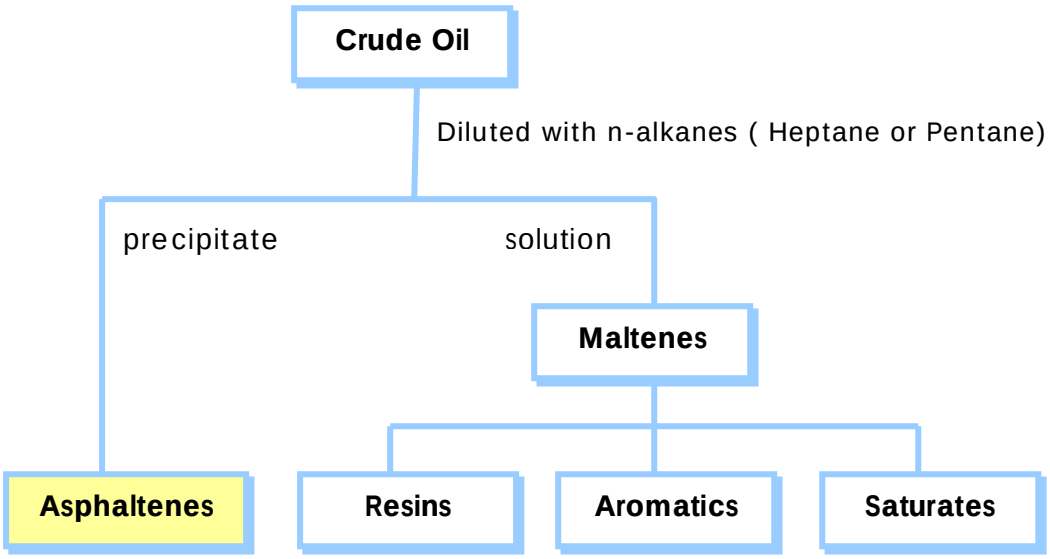

Figure 2.4 Composition of crude oil divided into SARA fractions [15]

Decreasing pressure (pressure depletion) will increase the relative volume fraction of the light components in crude oil. It causes an increase in the solubility parameter difference between crude oil and asphaltenes.

Asphaltene precipitation and deposition is one of serious potential problems during production, as it causes plugging of formation, wellbore, tubing and production facilities. It affects all aspect of petroleum production, processing and transportation[23].

2.3 Mechanism of Asphaltene Precipitation and Deposition

It is essential to distinguish term of precipitation and deposition, what the difference between them. Precipitation can be defined as the solid phase formation (fines) that comes out from a liquid phase while the deposition is described as the formation of precipitated solid phase on the surface.

Generally speaking, precipitation does not entirely lead to deposition process but deposition is typically affected by precipitation. The process of asphaltene precipitation is primarily a function of pressure, temperature and oil composition, while the deposition occurs after precipitation of asphaltene depending upon its attraction of fines to adsorb onto the surface. The process of fines aggregation into larger particles (flocs) is defined as flocculation. These flocs could break up into fines again totally or partially, which is called as process of flocs dissociation.

During deposition, the flocs are obtained from solution (oil phase) onto rock surface due to adsorption. The flocs could adsorb on the rock as static deposit, could block the pore throat (plugging) due to their bigger size compared to pore diameter or could be entrained and returned back into fines (dissolved in oil phase) due to high shear rate.

The deposition of asphaltenes will be severe problems on production because it triggers formation damage which reduces effective mobility of hydrocarbon[24] in terms of a significant reduction on porosity and effective rock permeability[25]. Not only that, the viscosity of oil increases as well and there is alteration of formation wettability from water-wet becomes more oil-wet rock[26].

As discussed above, the following diagram shows the mechanism of how asphaltenes make formation damage and what key parameters take part in this mechanism is depicted in Figure 2.5.

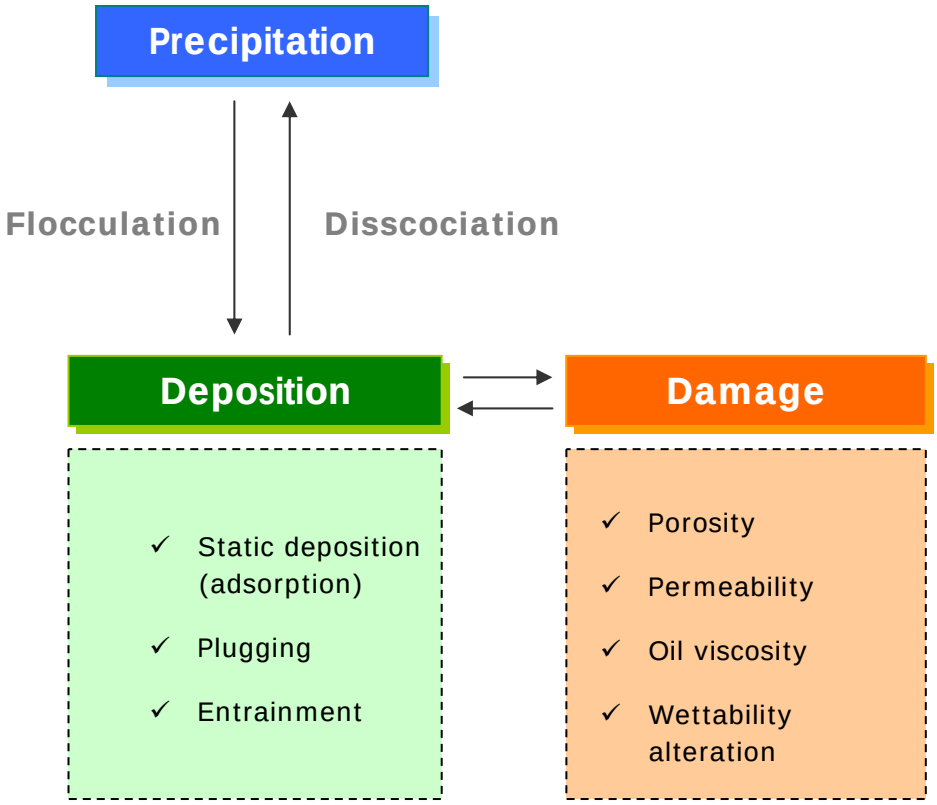

Figure 2.5 Mechanism of formation damage due to asphaltene precipitation and deposition processes

2.4 Practical Methods and Laboratory Works to Detect Asphaltene Precipitation

Many Industries have frequently used various practical techniques to study asphaltene precipitation. The common techniques that have proven fruitfully to detect asphaltene precipitation are listed in the following:

1. De Boer Plot

This method (plot) is proposed by De Boer and Leeriooyer[27] to identify at which condition crude oil has potential to cause flow assurance problems. In other word, this technique can be the first screening tool for categorizing the possibility of oil to demonstrate solid phase problems.

The De Boer Plot is constructed from data of laboratory experiments and various field experiences which divide into three regions (as shown in Figure 2.6):

- Region A with potential of severe problems
- Region B with moderate problems
- Region C with small or no problems

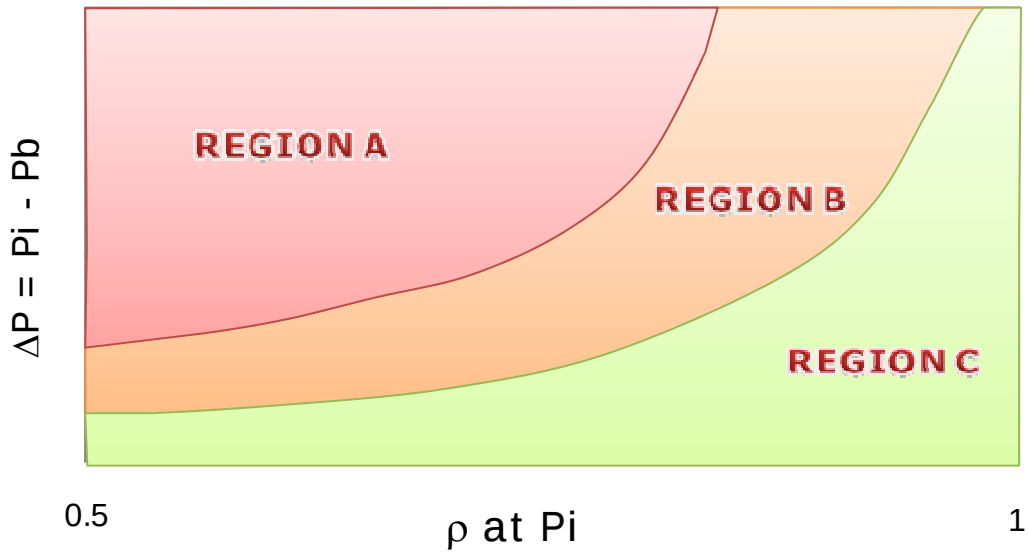

Figure 2.6 De Boer Plot

A De Boer Plot shows the relationship between pressure difference of initial pressure (Pi) and bubble-point pressure (Pb) on the y-axis and density of crude oil at initial pressure condition on the x-axis.

As well known from many literatures, the abundant of asphaltene deposits problems mostly occur at near or bubble-point pressure condition.

2. Asphaltene resin ratio approach

Jamaluddin et al[28] proposed different approach using asphaltene and resin ratio. The idea is to identify at what ratio of asphaltene by resin that may lead to asphaltene deposition problems. Figure 2.7 determines two regions such as stable and unstable region.

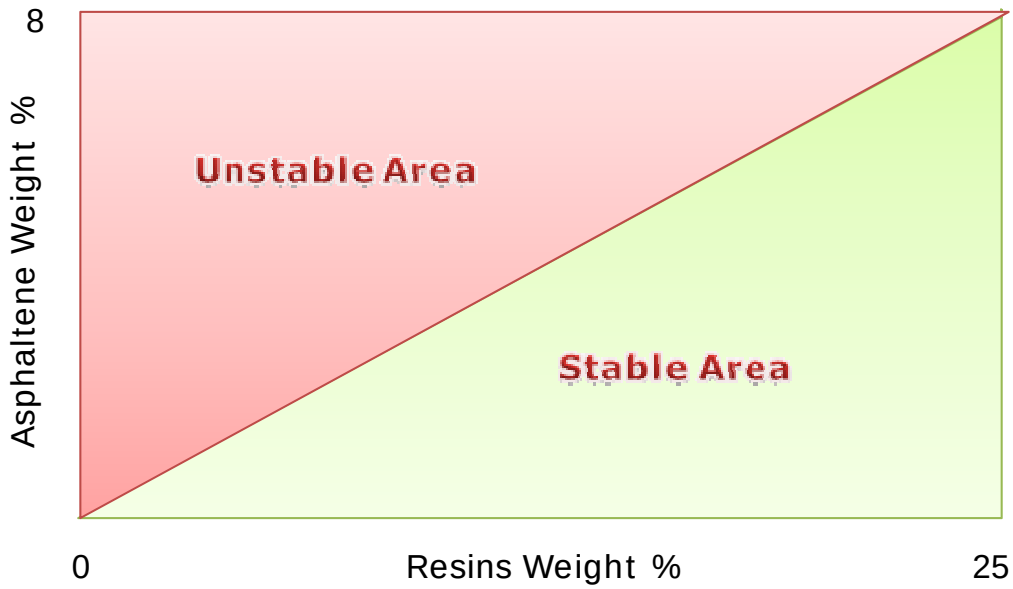

Figure 2.7 Relationship between asphaltene and resin weight percent

3. Colloidal Instability Index (CII)

CII value is another approach to identify crude oil system with having asphaltene deposit problems. This approach is suggested by Yen, Yin and Asomaning[29] where CII value expresses the ratio of the total asphaltenes and saturates to the total of aromatics and resins, which CII value ranges are simply categorized into three parts.

If oil has CII value below 0.7, it is defined as stable, whereas the CII higher than 0.9 is considered as unstable. For better illustration, Figure 2.8 presents in which area the oil is stable, mild or unstable with asphaltene deposit problems in terms of CII value.

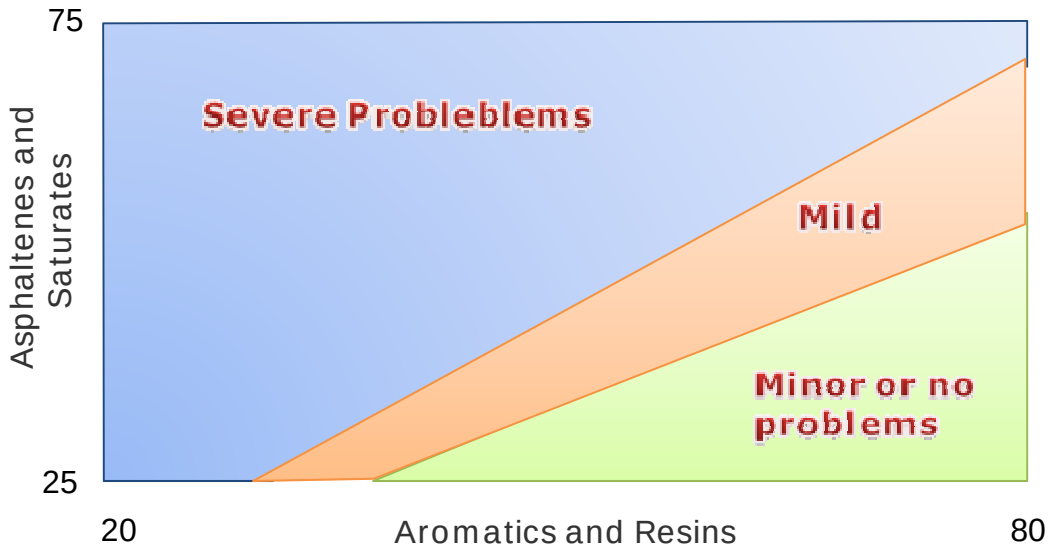

Figure 2. 8 Colloidal instability Index could be used to determine area where asphaltene deposits problems occur

Those practical methods are considered as a preliminary screening analysis for asphaltene deposit problems. It is strongly recommended to have further studies on laboratory experiments to clarify the potential problems. The common laboratory works which are frequently applied to measure asphaltene deposition are:

1. Gavimetric Method

In the gravimetric method, asphaltenes precipitate and fall to the bottom of a pressure-volume-temperature (PVT) cell. This method relies on the selected pressure steps. The output of this method is a plot of asphaltene concentration against pressure showing a transition period that corresponds to the upper and lower phase boundaries of asphaltene precipitation (as shown in Figure 2.9). The limitation of this method is prejudiced in determination of asphaltene onset precipitation because the measurement depends on the accuracy of the chosen pressure steps (magnitude of pressure interval). The onset points may be missed if the pressure interval too large. In other hand, a smaller interval for pressure measurement needs a time-consuming experiment and a massive volume of reservoir fluid.

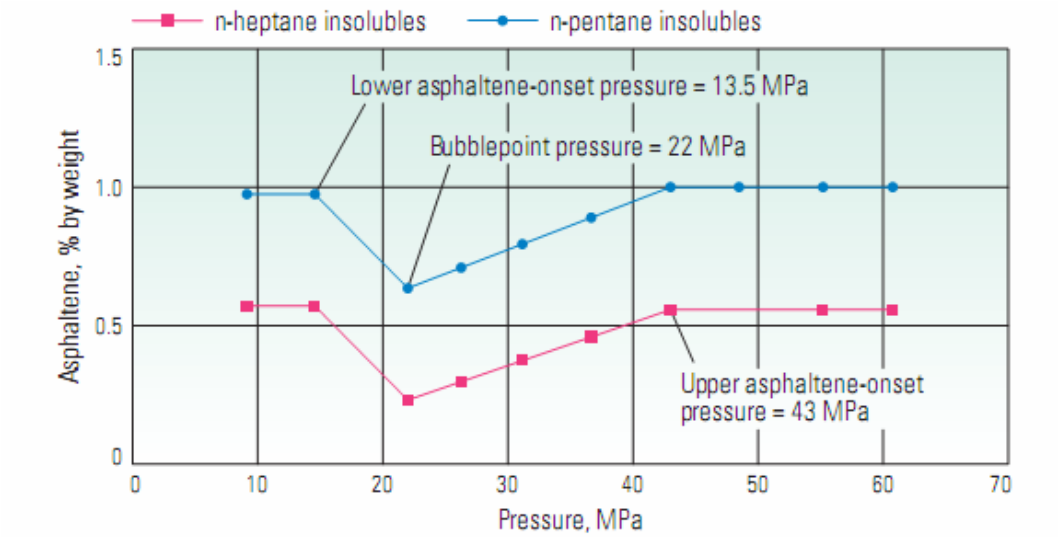

Figure 2. 9 A typical output of gravimetic technique to determine onset of asphaltene precipitation (figure taken from Schlumberger OilField Review magazine[2, 28])

From figure above, asphaltene starts to precipitate at pressure of 43 MPa, namely upper asphaltene onset pressure (upper AOP). The asphaltene contents in liquid drop continuously as pressure decreases until reaching a bubble point pressure at 22 MPa. At bubble point pressure, as pressure is further reduced, the dissolved gas that comes out from the liquid increases the solubility of asphaltene, so that asphaltene contents rise while pressure declines until achieves stabilization at pressure of 13.5 MPa. This pressure is called as lower AOP, which represents a point where precipitation process stops.

Those conditions are illustrated in figure 2.10, which shows basically a qualitative amount of asphaltene precipitation at different conditions (pressure) where black dots represent the quantity of precipitated asphaltene.

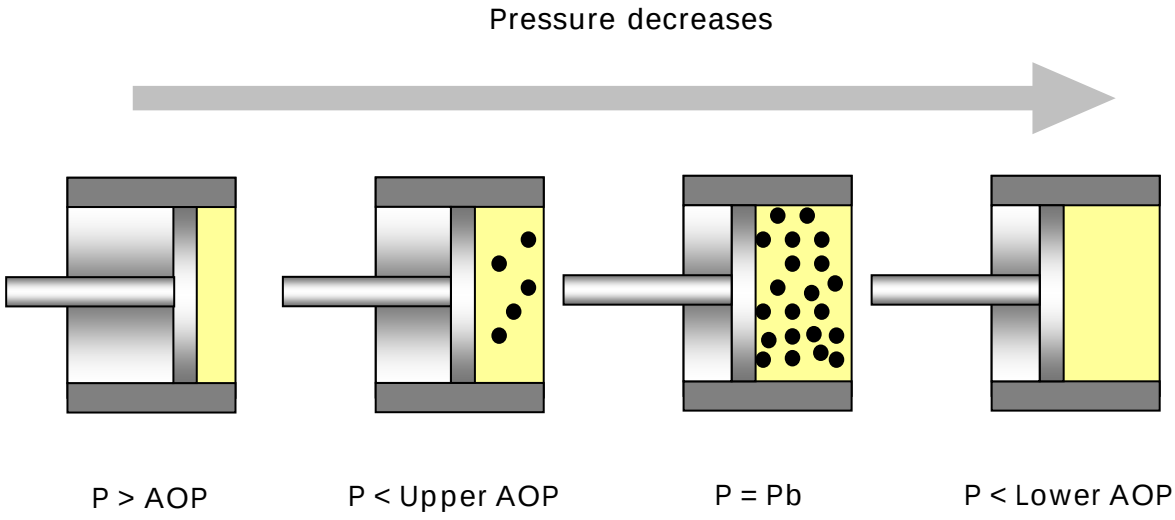

Figure 2. 10 Schematic demonstrates asphaltene onset pressure governs at which condition asphaltene begins to precipitate and redissolve into liquid[2]

As shown in the figure above, it can be clearly understood that when pressure is higher than upper AOP, no precipitation of asphaltene occurs in the beginning, but since the pressure at upper AOP, asphaltene starts to precipitate and the amount of precipitated asphaltene rises and reaches a maximum at bubble point pressure. At pressure less than bubble point pressure, light components of oil evolves, ~~so~~ asphaltene becomes more soluble again, it means that there is a redissolution process of the prior precipitated asphaltene. A precipitation process will not proceed anymore if pressure is below lower AOP.

2. Acoustic Resonance Technique (ART) Method

The objective of this method is to measure changes in the acoustic fluid properties while asphaltene drops out from the solution. Compared to a gavimetric method, this technique consumes less time of work. On the other side, a similar observation in acoustic properties can be shown for both situations whether due to presence of other solids or vapor-liquid phase boundaries. A major drawback of the ART method is detection of resonance changes are not unique, furthermore, the lower boundary of asphaltene precipitation envelope can not be detected because of gradual phase transition in asphaltene dissolution process.

or instance, figure 2.11 shows how an acoustic receiver used in the ART method detects acoustic resonance which is emitted by an acoustics transducer.

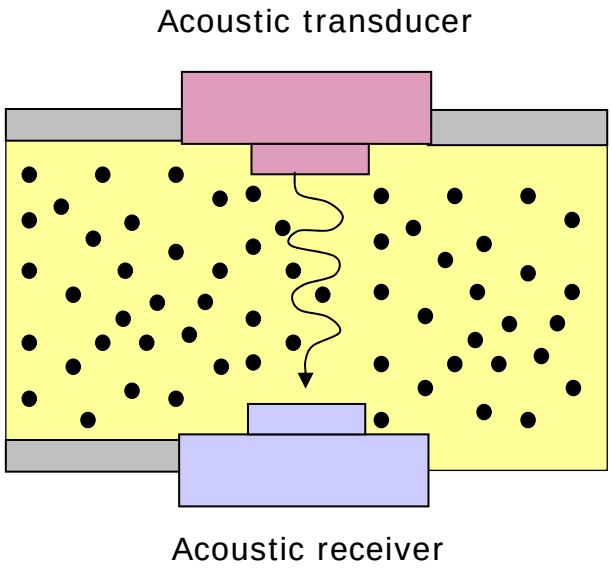

Figure 2.11 Schematic of acoustic resonance technique to detect asphaltene precipitation[2]

Asphaltene onset pressure (AOP), only the upper AOP, can be obviously shown from the output chart generated by the ART (see figure 2.12). During depressurization, a sharp drop in acoustic responses are detected representing the upper AOP, at the first observation, and the following drop corresponds to bubble point pressure. The figure depicted shows upper AOP and bubble point pressure from the ART method which has a similar detection obtained by a gravimetric method (see figure 2.9).

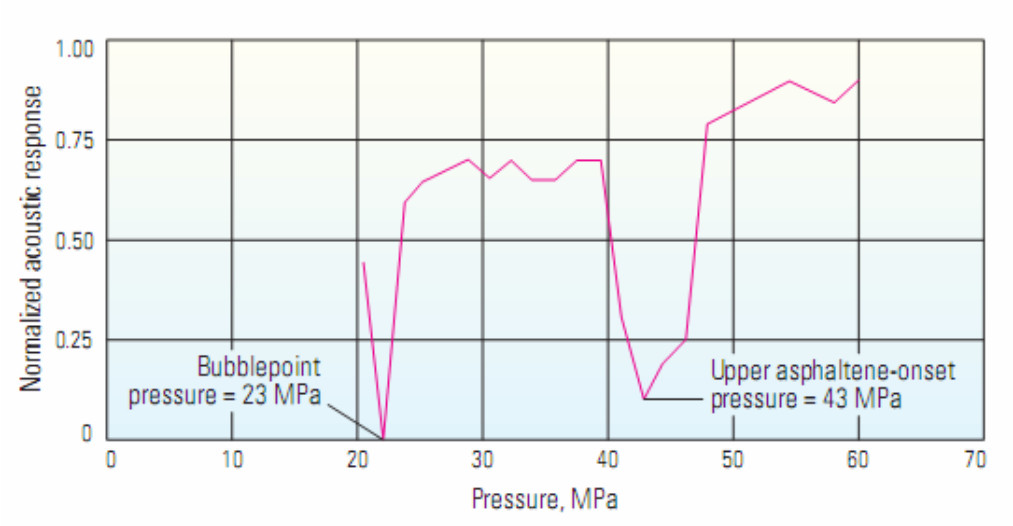

Figure 2.12 A typical output of acoustic resonance technique to detect upper asphaltene onset pressure (figure taken from Schlumberger OilField Review magazine[2, 28])

3. Light Scattering (LST) Method

Another name for this method is solids-detection system (SDS). The LST uses near-infrared light to probe fluids as asphaltene precipitates either at isothermal depressurization or at isobaric with decreasing temperature. The principle is a near-infrared light source on side of the cell generates light and when asphaltene precipitate, the light is scattered and the transmittance power of the light is also reduced. This transmittance power of light is detected by fiber-optic sensors located at other side of the cell. For further detail, the illustration of the LST is given in figure 2.13 below.

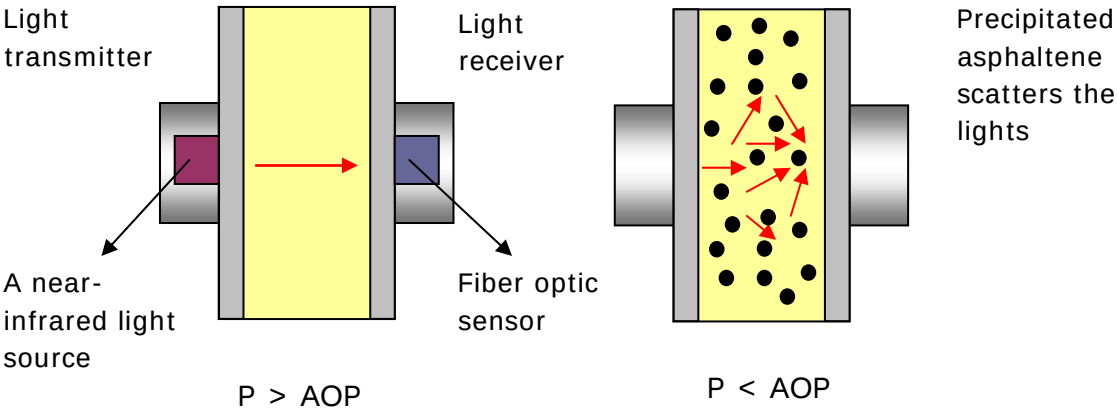

Figure 2.13 An illustration of the light-scattering technique when pressure is below AOP the light is scattered

A typical response of output from the LST method shows complete asphaltene precipitation envelope, particularly the detection of upper AOP, bubble point and lower AOP that can be visibly determined (see figure 2.14). As pressure decreases, the light transmittance power increases due to denser fluid which gives more light transmission. When asphaltene precipitates because pressure is across upper AOP, a significant drop of light transmittance power occurs. At bubble point pressure, the gas is more dropping out from the solution as decreasing pressure, this make increase in light transmission. The lower AOP can be marked by a jump response of light transmission which indicates asphaltene start to redissolve, known as lower AOP.

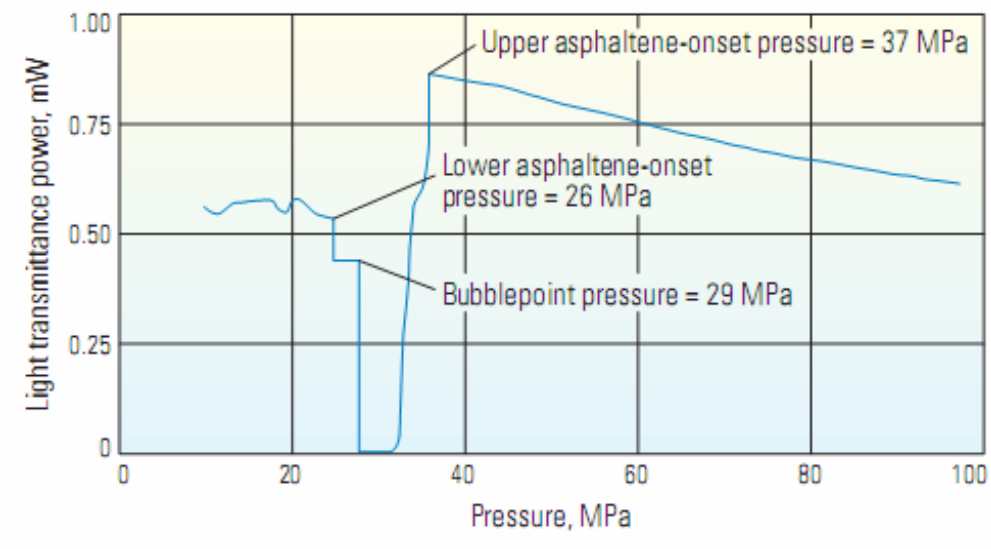

Figure 2. 14 A typical output of the light-scattering technique that is able to detect upper AOP, bubble point and lower AOP with respect to the light transmission (figure taken from Schlumberger OilField Review magazine[2, 28])

4. Filtration Method

A filtration method uses a PVT cell filter to extract the fluid passing during depressurization in order to quantify the amount of precipitated asphaltene. The advantage of this technique is that asphaltene is physically extracted from oil and then may further be studied using other techniques such as saturated, aromatic, resin and asphaltene (SARA) analysis. However, the results of this process depend on filter size used.

2.5 Asphaltene Behavior Modeling

To have full understanding of asphaltene behavior, it is necessary to look at a wider range of conditions compared to laboratory experiments. Due to limitation in experiment conditions, the outcomes are probably obtained at selected conditions (at particular pressure, temperature and composition) which may not address the sensitivities analysis of each parameter because of time and tool constraints. By having full range of conditions on asphaltene behavior will lead to better knowledge on which parameters have the most influence on asphaltene behavior.

The product of experiments will be used as validation for a model used. After tuning the model, the following step is to generate additional performances corresponds to given parameters.

In general, there are four models which have been reported and frequently referred to in literature to model asphaltene behavior: solubility models, solid models, colloidal models and association equations of state (EOS) models.

1. Solubility models

The first concept of solubility model was developed by Flory[30] and followed then by Hirschberg[11] to describe asphaltene stability by considering the reversibility of solution equilibrium. This model becomes most regularly approach to predict asphaltene precipitation.

Some researchers improved the model with extra focus by taking the effect of gas phase into account and then proposed three phase equilibrium[31]. In 1995, Cimino[32] included polymer solution thermodynamics into computation which leads to be more representative for modeling asphaltene behavior as long as the model is calibrated by experimental data.

Burke[5],Novosad an Costain[33] and Kokal et al[34] tried to match this model by experimental results with some degree of success.

2. Solid models

A solid model is the simplest model because it treats precipitated asphaltene as a single component (solid phase) whereas oil and gas phases are determined by a cubic equation of state. This model involves an introduction of many parameters of tuning in order to validate the model with experimental data. A solid model assumes the heavy ends of oil are divided into two parts: precipitating (asphaltene) and non-precipitating components (resin)[7].

Chung et al[35] proposed a solid model treating asphaltene as a lumped pseudocomponent and rest components are solvent. Chung et al's model is much simple and the model performs a direct computation of asphaltene stability. Nevertheless, pressure is not taken into account; in fact, pressure is well understood as an important factor of asphaltene stability.

3. Colloidal models

At the first time, a previous model focused on molecular thermodynamics and assumed at situation where a process of asphaltene/resin precipitation is unaffected. In 1987, Leontaritis and Mansoori[9] proposed another approach where asphaltene is considered as solid particles in colloidal suspension stabilized by adsorbed resins on asphaltene's surface.

A vapor-liquid equilibrium is calculated by an EOS which produces a composition of liquid phase at which region asphaltene will flocculate. Based on experimental measurement of onset of precipitation at particular condition, the critical chemical potential of resin is estimated by using Flory-Huggins polymer solution theory and this value is subsequently used to predict at other conditions.

4. Association equations of state models

The recent EOS is a statistical associating fluid theory (SAFT). In 1989, Chapman et al[36] developed an EOS model to predict phase equilibria based on SAFT. Paricaud et al[37] in 2002 applied the use of SAFT to model the limit of polymer–colloid system stability. Moreover, Chapman et al[38] proposed an improved model which considers the effect of molecular shape, van der wals interaction and effects of intramolecular association. This model has demonstrated an accurate prediction to more complex fluid systems. In 2007, a PC-SAFT EOS has been proposed by Pedersen and Hasdbjerg[8] which can be applied to petroleum reservoir fluids. The PC-SAFT model has been proven and tested to handle ~~for~~ of various types of petroleum fluid systems from natural gas to heavy oil mixtures with asphaltene.

CHAPTER 3 DATA AND METHODOLOGY

To be systematic and well documented, this chapter will be divided into two main sections to distinguish which type of methods are used to model asphaltene precipitation either using equation or a simulator. Each section will provide all required data, procedures or flowcharts, assumptions taken and calculation results.

3.1 Model Description

In the following section, the proposed approach considers pressure, temperature and also changes in oil composition due to CO_2 injection.

A simple model for asphaltene precipitation is introduced based on the polymer solution model. It is considered that the polymer solution can represent asphaltene precipitation and dissolution processes in oil compared to other models.

Hirschberg et al[11] expressed equation 3.1 for the maximum volume fraction of dissolved asphaltene in liquid (oil):

$$\phi_A^{\max} = \exp\left[\frac{MV_A}{MV_L} - 1 - \frac{MV_A}{RT}\left(\delta_A - \delta_L\right)^2\right] \tag{3.1}$$

Where:

$\phi_A^{\max}$ = maximum volume fraction of dissolved asphaltene in liquid

MV_A, MV_L = molar volume of asphaltene and liquid, respectively

R = universal gas constant

T = temperature

δ_A, δ_L = solubility parameter of asphaltene and liquid, respectively

Equation above was derived with an assumption that the precipitated phase is pure asphaltene.

Weight fraction of precipitated asphaltene ($W_{AF)}$ is calculated using equation 3.2. The weight of precipitated asphaltene (W_A) depends upon weight of asphaltene remains in the liquid (W_{AL}).

$$W_{AF} = \frac{W_A}{W_{TL}} = \frac{\left(W_{TAL} - W_{AL}\right)}{W_{TL}} \tag{3.2}$$

Where:

W_A = weight of precipitated asphaltene

W_{TAL} = maximum weight of asphaltene in liquid

W_{AL} = weight of asphaltene in liquid after flooding

W_{TL} = total weight of liquid

Volume fraction of precipitated asphaltene (V_{AF}) and asphaltene in the liquid (V_{AL}) is defined by equation 3.3 and equation 3.4, respectively.

$$V_{AF} = \frac{V_A}{V_{TL}} = \frac{\left(\frac{W_A}{\rho_A}\right)}{\left(\frac{W_{TL}}{\rho_L}\right)} = \frac{W_A}{W_{TL}}\left(\frac{\rho_L}{\rho_A}\right) = W_{AF}\left(\frac{\rho_L}{\rho_A}\right) \tag{3.3}$$

$$V_{AL} = \frac{V_{TL} - \frac{\left(W_{TL} - W_{AL}\right)}{\rho_A}}{V_{TL}} \tag{3.4}$$

V_A and V_{TL} denote volume of precipitated asphaltene and total volume of liquid, respectively. ρ_A and ρ_L are defined as density of asphaltene and liquid, respectively.

Equation 3.4 can be re-written in equation 3.5 to determine the total weight of liquid.

$$W_{TL} = \left(V_{TL} - V_{TL} * V_{AL}\right)\rho_A + W_{AL} \tag{3.5}$$

V_{AL} is defined as volume fraction of dissolved asphaltene in liquid. W_{AL} denotes weight of asphaltene remains in liquid.

A final equation to calculate weight percent of precipitated asphaltene is obtained by combining equation 3.2 and 3.5.

$$W_A\% = \frac{\left(W_{TAL} - W_{AL}\right)}{\left(V_{TL} - V_{TL} * V_{AL}\right)\rho_A + W_{AL}} * 100 \tag{3.6}$$

By applying a Flory-Huggins polymer-solution theory and Hildebrand solubility concept (δ) in equation 3.6, a volume fraction of dissolved asphaltene in liquid (V_{AL}) can be calculated. Therefore, the weight percent of precipitated asphaltene in terms of solubility parameters can be expressed as follows:

$$W_{\text{model}} = \frac{\left(W_{TAL} - W_{AL}\right)}{\left(V_{TL} - V_{TL} * \exp\left(\frac{MV_A}{MV_L} - 1 - \frac{MV_A}{RT}\left(\delta_A - \delta_L\right)^2\right)\right) * \rho_A + W_{AL}} * 100 \tag{3.7}$$

Where:

W_{model} = weight percent of precipitated asphaltene (%)

W_{TAL} = maximum weight of asphaltene in liquid (gram)

W_{AL} = weight of asphaltene in liquid after flooding (gram)

V_{TL} = total volume of liquid (cm^3)

MV_A = molar volume of asphaltene (cm^3/mol)

MV_L = molar volume of liquid (cm^3/mol)

δ_A = solubility parameter of asphaltene($MPa^{1/2}$)

δ_L = = solubility parameter of liquid ($MPa^{1/2}$)

R = universal gas constant (8.314472 MPa cm^3 mol^{-1} K^{-1})

T = temperature (K)

ρ_A = density of asphaltene (1.28 gram/cm^3)

Density of asphaltene is taken as constant value 1.28 gram/cm^3 for simplicity refers to Andersen and Speight[39].

Hirschberg et al[11] defined solubility parameter of asphaltene (δ_A) as a function of temperature which is expressed by equation 3.8.

$$\delta_A = 20.04 * \left(1 - 1.07 * 10^{-3} * T(C)\right) \tag{3.8}$$

Solubility parameter of liquid is the main subject on this study since this parameter is believed as internal cohesive density parameter (CED) which is known as the molar internal energy of vaporization of pure liquid (ΔU_{vap}) divided by its molar volume (MV_L).

$$\delta_L = CED^{1/2} = \sqrt{\frac{\Delta U_{vap}}{MV_L}} \tag{3.9}$$

Johansson et al[40] developed an approximation of molar internal energy of vaporization as a function of boiling temperature (T_b).

$$\Delta U_{vap}(J/mol) = -14820 + 99.2 * \mathrm{T_b(K)} + 0.084 * \mathrm{T_b(K)}^2 \tag{3.10}$$

An adjustment to the solubility parameter of liquid is required so that the model becomes unique solution for specific oil sample. Therefore, α and β are introduced as tuning parameters and molar volume of CO_2 (MV_{CO2}) is incorporated into the equation to address the effect of CO_2 injection. The best fit of function for the solubility parameter of liquid is given in equation 3.11.

$$\delta_L = \alpha * \sqrt{\frac{\Delta U_{vap}}{MV_L}} * \exp\left[\left(\frac{MV_{CO2}}{MV_L}\right)^{\beta}\right] \qquad (3.11)$$

Tuning parameters α and β are determined by non-linear regression method corresponding to the experimental results. These tuning parameters are constant for specific oil sample.

3.1.3 Procedures of Computation

Interest area of work on modeling asphaltene behavior is to calculate how much precipitated asphaltene at any pressures, temperatures and compositions (due to injected CO_2).

The original oil compositions were taken from literatures is then recombined with CO_2 at experiment conditions (specific pressure and temperature). By varying values of mol% CO_2, a new composition of recombined mixture will be created. In this study, PVTsim is used to generate PVT properties required in computation as pressure, temperature and composition changes.

The following PVT data are important to be updated correspond to different circumstances given:

Condition 1: Changes in pressure and temperature at particular recombined mixture

- Density of liquid (ρ_L)
- Molar volume of liquid (MV_L)

– Molar volume of pure CO_2 (MV_{CO2})

– Boiling temperature (T_b)

Condition 2: Changes in composition (another recombined mixture)

– Total weight of liquid (W_{TL})

– Total weight of asphaltene (W_{TAL})

W_{TL} and W_{TAL} are assumed constant for any pressures and temperatures (mass conservation)

Figure 3.1 describes process flow of calculations step by step. As seen in the figure, the model initially estimates weight percent of precipitated asphaltene at experiment conditions (specific pressure and temperature). The model is subsequently validated by set of experimental data to determine tuning parameters (α and β).

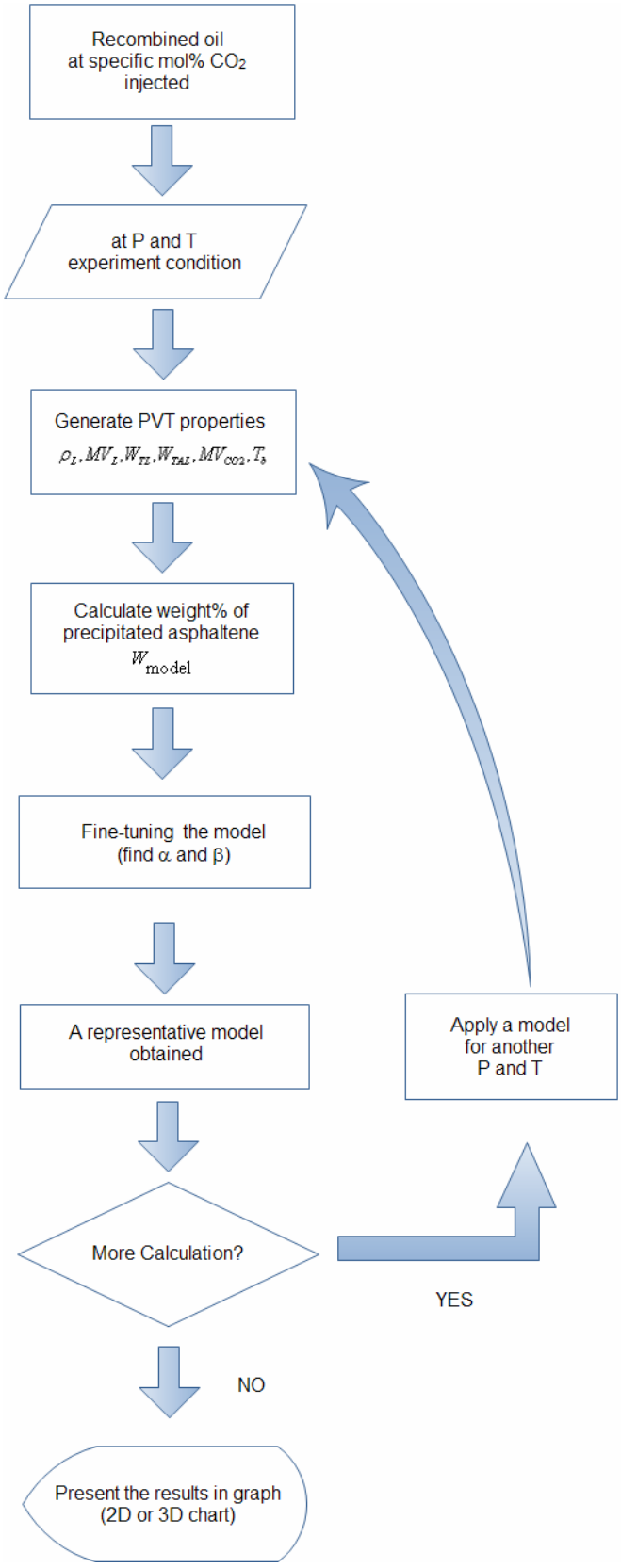

Figure 3.1 Process flow of computations

In order to solve the unknowns of tuning parameters, the fitting process of model is considered in an iterative manner as shown in figure 3.2. Iteration process will stop when the residual error is less than convergence criteria (ε). When the iterations are complete, best fit of tuning parameters are found and the representative model is ready to use in the simulation.

Prior to the simulation, most of the PVT properties as mentioned previously must be generated at different pressures and temperatures. By simulating sets of combination of pressure and temperature, weight percent of precipitated asphaltene can be estimated in wide ranges of operating conditions so that a better understanding of asphaltene behavior can be attained.

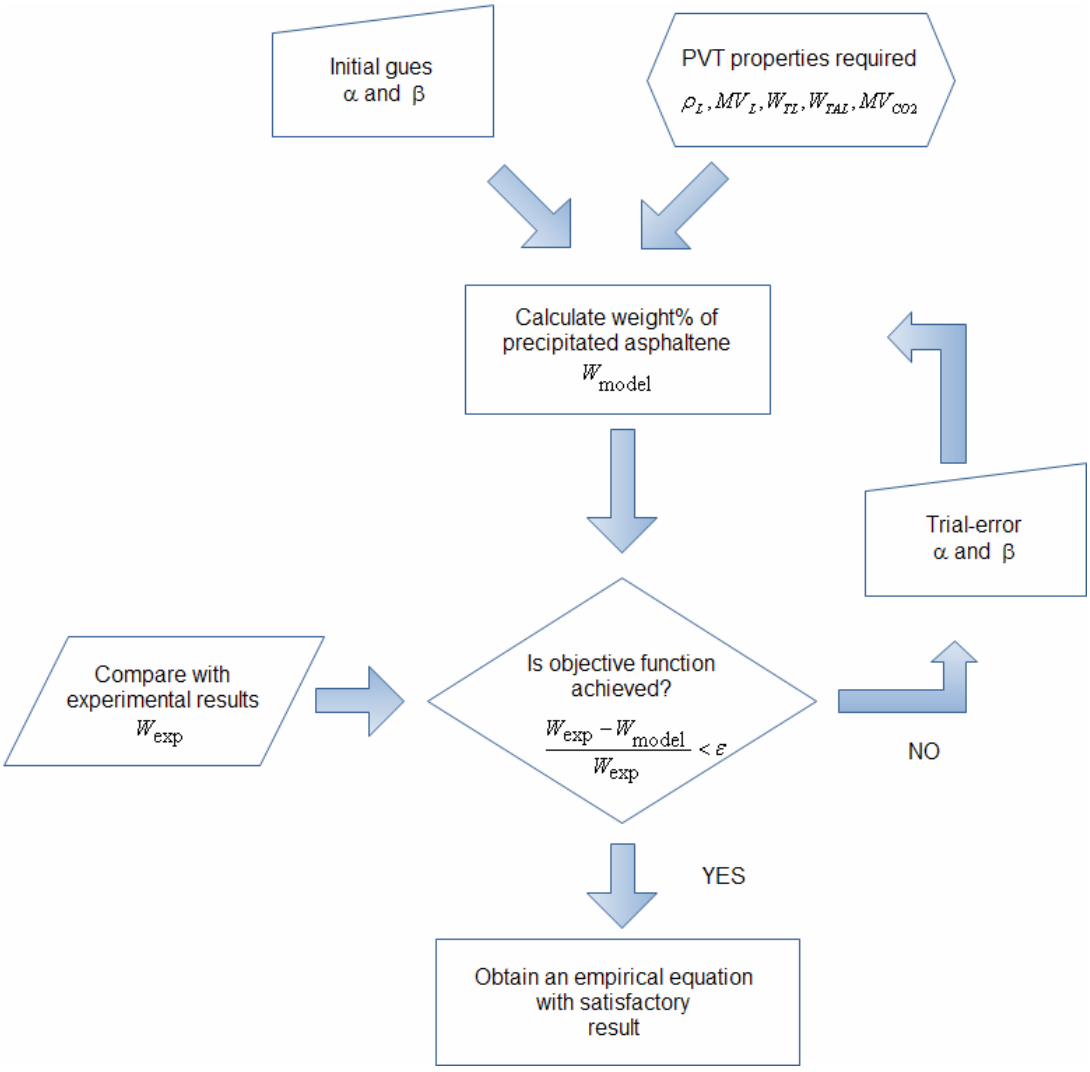

Figure 3.2 Model fitting (validation) diagram

During computation, density of asphaltene is assumed to be constant (1.28 g/cm^3) regardless at which pressure, temperature and composition are applied. For molar volume of asphaltene, at specific oil sample this value is kept constant at any pressures and temperatures.

Because of many variables are involved, outline of formulas are illustrated in figure 3.3 to show the relationship among variables and breakdown which PVT properties must be updated when pressure, temperature and composition are changed.

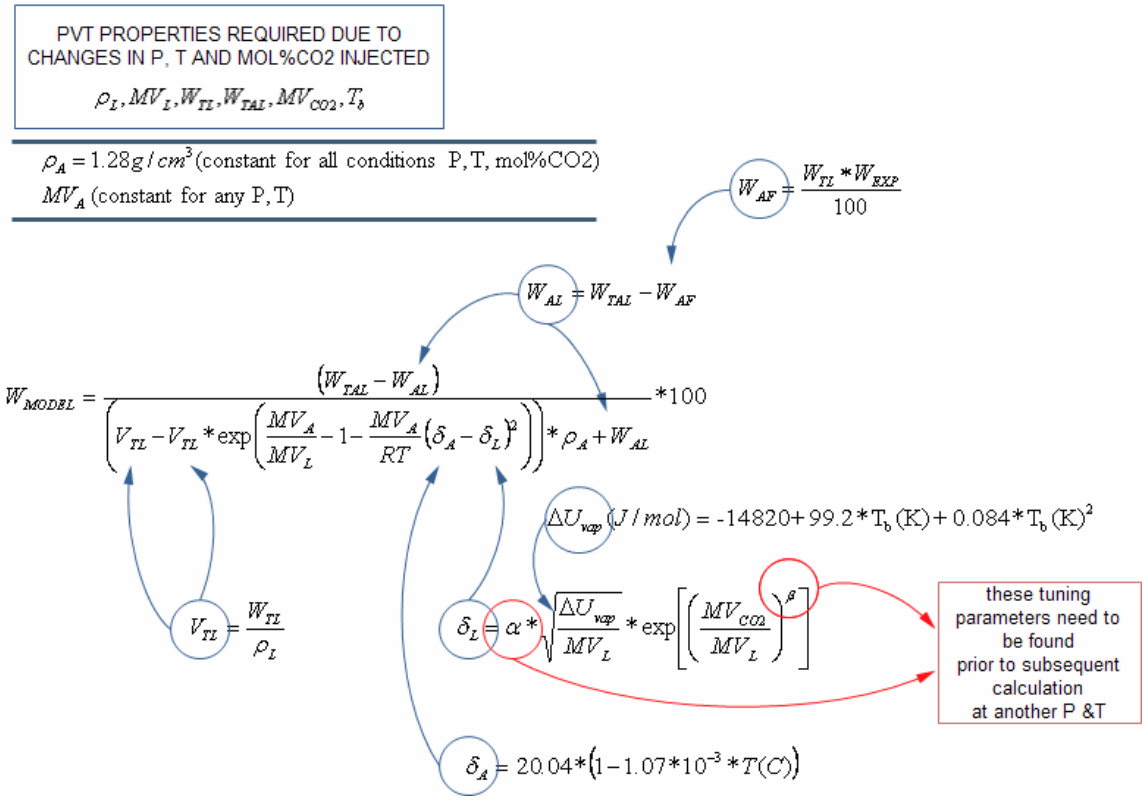

Figure 3.3 Outline of equations used in computation and relationship among variables

3.1.4 Experimental Data (Literature)

Several experimental results are used to develop and validate the model. Only literatures presented measurements of precipitated asphaltene with various concentrations of CO2 injection are chosen

in this thesis. The following conditions of experiments are given in table 3.1.

Table 3.1 Experiment conditions for different literatures

Literature	Pressure (bar)	Temp (deg C)
Vafaie Sefti et al	150	99.85
Hu et al	150	65.85

A recombination of oil with CO_2 is performed by using PVT software (PVTsim) to generate the altered oil composition for each mol% of CO_2 injected. The recombined oil compositions both literatures are presented in appendix A.

Table 3.2 and 3.3 show the original oil composition of Vafaie et al and Hu et al, respectively. In addition, table 3.4 and 3.5 present the experimental results of weight percent of precipitated asphaltene during CO_2 injection for Vafaie et al and Hu et al, respectively.

Table 3.2 Oil composition with 0% CO2 injection (Vafaie Sefti et al)

Component	Mol %	MW	ρ_L (g/cm^3)
N2	0.570	44.010	
CO2	2.460	28.014	
C1	36.366	16.040	
C2	3.470	30.070	
C3	4.050	44.097	
i-C4	0.590	58.124	
n-C4	1.340	58.124	
i-C5	0.740	72.151	
n-C5	0.830	72.151	
C6	1.620	86.178	0.6640
PS1	18.198	142	0.8680
PS2	13.979	274	0.8730
PS3	3.690	350	0.8770
Resin	8.929	603	1.0000
ASP	3.170	850	1.2800

Table 3.3 Oil composition with 0% CO2 injection (Hu et al)

Component	Mol%	MW	ρL (g/cm3)
N2	0.960	44.010	
CO2	0.160	28.014	
C1	24.060	16.040	
C2	0.760	30.070	
C3	3.260	44.097	
i-C4	0.640	58.124	
n-C4	2.700	58.124	
i-C5	0.520	72.151	
n-C5	1.060	72.151	
C6	0.700	86.178	0.6640
C7	0.580	91.26	0.7380
C8	1.860	104.27	0.7650
C9	2.300	118.97	0.7810
C10	0.820	175	0.7920
C11+	52.910	442	0.9215
Resin	4.890	850	1.0000
ASP	1.820	1000	1.2800

Table 3.4 Experimental results of weight percent of precipitated ashaltene with various mol% CO2 injected (Vafaie Sefti et al)

Mol% of CO2 injected	Mol% of CO2 in liquid	Weight% of precipitated asphaltene (W_{EXP})
2.4942	4.039	0.789474
11.5012	10.146	4.52632
18.9838	14.271	7.05263
25.2194	17.177	8.68421
30.485	19.31	9.73684
35.0577	20.976	10.3684
40.0462	22.619	10.7895
42.5404	23.391	11.1053
46.0046	24.385	11.2632
48.77	25.136	11.3158

Table 3.5 Experimental results of weight percent of precipitated ashaltene with various mol% CO2 injected (Hu et al)

Mol% of CO2 injected	Mol% of CO2 in liquid	Weight% of precipitated asphaltene (W_{EXP})
51.6	32.251	0.06
63.8	35.875	0.23
71.6	37.744	0.32
80.2	39.463	0.42

3.2 Compositional Simulation

The simulator ECLICPSE^{TM} is applied to a reservoir of 7500 ft long, 1000 ft width and 50 ft thick which is located at a depth of 4000 ft. The simulated reservoir has a dimension of 15 x 1 x 1 (1-D horizontal) where an injector is located at block 1 (left edge of block) and the other boundary is producer (see figure 3.4).

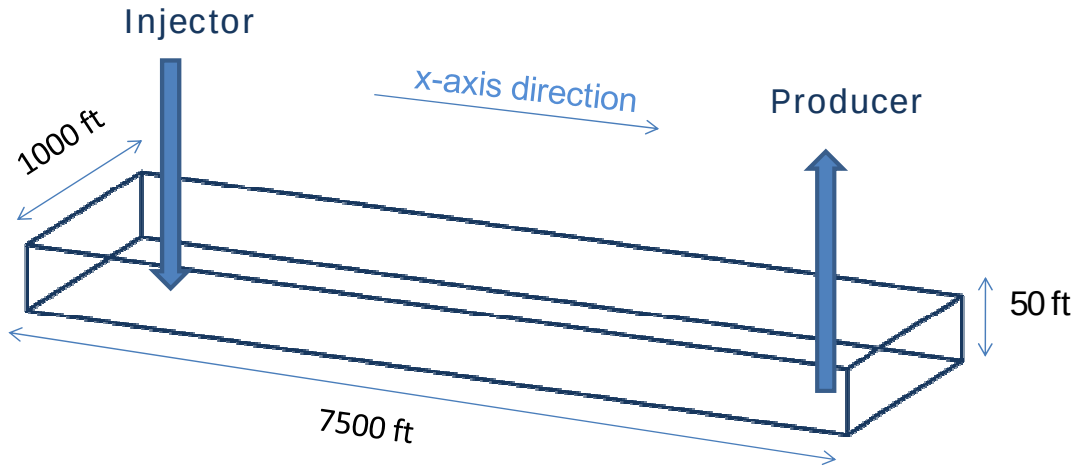

Figure 3.4 Block dimensions of simulated reservoir with grid 15 x 1 x 1

The reservoir is divided into 15 blocks with a block length of 50ft at the first and the last three blocks and 800ft in between. Initial reservoir pressure (P_i) is 4000 psia. Gas-oil contact (d_{GOC}) is located at depth of 2000 ft while oil-water contact (d_{WOC}) at 4060 ft.

The absolute permeability is 500 md and fractional porosity is 0.1. The initial oil saturation is 0.84. A reservoir rock compressibility is set to 3.5 10^{-6} psi^{-1}.

Table 3.6 Reservoir properties

Parameter	Value
Absolute porosity	0.1
Permeability	500 md
d_{GOC}	2000 ft
d_{WOC}	4060 ft
S_{oi}	0.84
P_i	400 psia
Reservoir fluids	Gas, oil, water
C_{rock}	3.5E-6

In this study, a reservoir fluid has 8 components which no presence of CO_2 in the mixture. Meanwhile, the mixture initially contains 2% asphaltene. All PVT properties and compostion of reservoir fluid are described in table 3.6.

Table 3.7 Reservoir fluid composition and PVT properties

Component	z_i	MW	Tcrit	Pcrit	Zcrit	ACF
CO_2	0	44.01	547.56	1069.867	0.27414	0.225
C1	0.5	16.04	343	667.8	0.29	0.013
C3	0.03	44.1	665.7	616.3	0.277	0.153
C6	0.07	86.18	913.4	436.9	0.264	0.301
C10	0.2	149.29	1111.8	304	0.257	0.489
C15	0.1	206	1270	200	0.245	0.65
C20	0.08	282	1380	162	0.235	0.85
ASPHALTENE	0.02	282	1380	162	0.235	0.85

The relationship of fluid flow among phases in the reservoir is governed by relative permeability curves (see in figure 3.5).

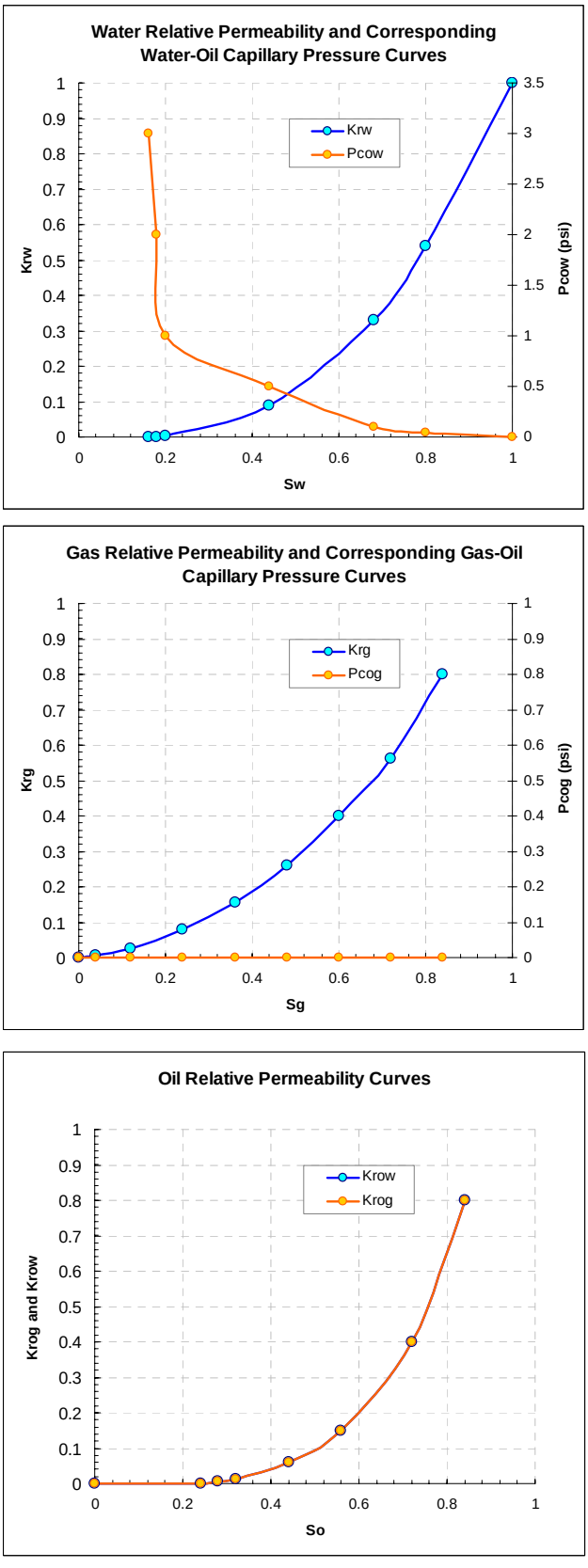

Figure 3.5 (a) water relative permeability curve as a function of water saturation (b) gas relative permeability curve as a function of gas saturation (c) oil-water and oil-gas relative permeability curves as a function of oil saturation

To be able to simulate asphaltene behavior, an ASPHALTE keyword must be activated. This keyword is only available in ECLIPSE 300 simulator (compositional model).

It has been informed that the 7th component (C_{20}) is the only component which has possibility to precipitate and flocculate into the 8th component (asphaltene). Table 3.7 describes flocculation and dissociation rates specified in simulation. In addition, deposition rate which is a function of adsorption, plugging and entrainment rates are given in table 3.8.

Table 3.8 Asphaltene flocculation and dissociation rates

Process	day^{-1}
C_{20} → Asphaltene	0.01
Asphaltene → C_{20}	0.0001

Table 3.9 Deposition rate components

Adsorption Coefficient (day^{-1})	Plugging Coefficient (ft^{-1})	Entrainment Coefficient (ft^{-1})	Vcrit (ft/day)
5.0E-3	1E-7	1.0E-7	2500

Constraints on bottomhole pressures and rates for producer and injector are described in table 3.10.

Table 3.10 Constraints taken for producer and injector

Target Production (RB/D)	Water Injector (RB/D)	CO_2 Injector (CFT/D)
3500	25000	15000

BHP of injector (upper limit)	BHP of producer (lower limit)
4400 psia	500 psia

CHAPTER 4 RESULT AND DISCUSSIONS

4.1 Modeling of Asphaltene Precipitation during CO_2 Flooding

By using the proposed equation, the amount of asphaltene precipitation with the presence of CO_2 can be predicted. The required inputs for this equation are the fluid compositions of recombined oil with CO_2 injected (appendix A), amount of precipitated asphaltene for different CO_2 injection by experiment (Table 3.4 and 3.5), and adjustment or tuning to match the model (equation).

4.1.1 Model validation with experimental data

An adjustment or a tuning process needs to be made to produce a representative model so that such model can be used to determine the amount of precipitated asphaltene.

The validation of model relies on the iterative technique of the tuning parameters α and β. In non-linear regression, how to match those parameters on matching the predicted values to experimental results is governed by sum of squares error (known as SSE). SSE is used as a basis to asses how well the model (equation) fits the experimental data. In order words, SSE represents the sum of squared deviations of actual values from predicted values as expressed in equation 4.1.

$$SSE = \sum_{i=1}^{n}\left[\left(W_{\text{exp}}\right)_i - \left(W_{\text{model}}\right)_i\right]^2 \qquad (4.1)$$

Trial-error of tuning parameters is essential to calculate the SSE values as illustrated in figure 4.1. By knowing the interest area of tuning parameters (as marked by dotted lines in figure 4.1), the ranges of tuning parameters α and β can be narrowed.

In this study, a Gauss-Newton method for iteration process was used. This iteration method strongly relies on the initial guess. Therefore, the narrowed ranges of tuning parameters (table 4.1) can be useful to obtain the smallest SSE.

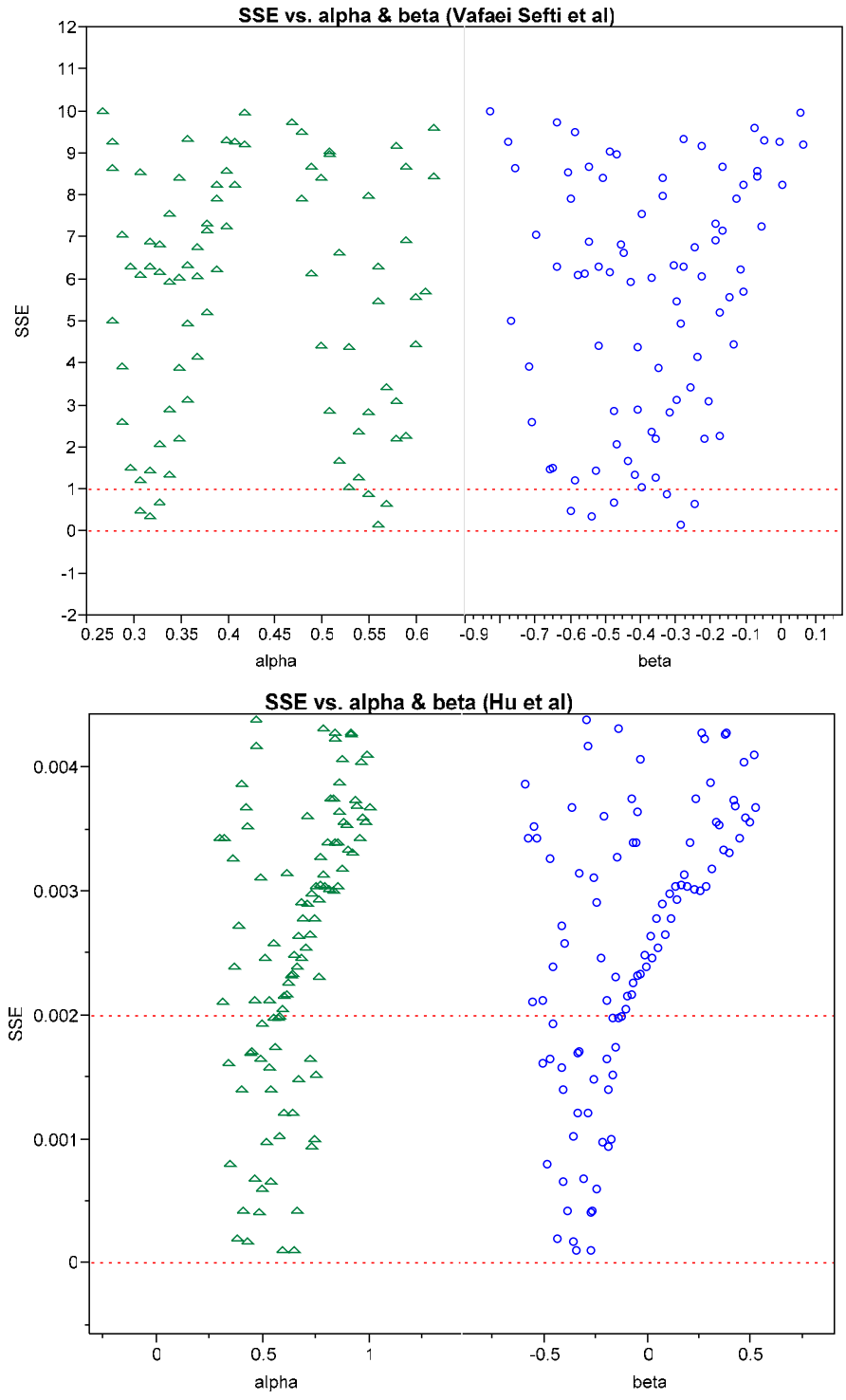

Figure 4.1 Combination of tuning parameters with respect to SSE produced for (a) Vafaei Sefti et al (b) Hu et al

Table 4.1 Interest area of tuning parameters (a) Vafaei Sefti et al (b) Hu et al

α	β	SSE
0.296482	-0.65829	1.483285
0.296482	-0.64824	1.488981
0.306533	-0.59799	0.492866
0.316583	-0.53769	0.335558
0.316583	-0.52764	1.446041
0.326633	-0.47739	0.682229
0.517588	-0.43719	1.674146
0.336683	-0.41709	1.337705
0.537688	-0.35678	1.280035
0.547739	-0.32663	0.862558
0.557789	-0.28643	0.140245
0.567839	-0.24623	0.650801

α	β	SSE
0.346734	-0.48744	0.000794
0.376884	-0.43719	0.000191
0.537688	-0.40704	0.000656
0.407035	-0.38693	0.000419
0.427136	-0.35678	0.00017
0.58794	-0.34673	0.000104
0.457286	-0.30653	0.000681
0.477387	-0.27638	0.000407
0.658291	-0.26633	0.000416
0.497487	-0.24623	0.00059
0.517588	-0.21608	0.000977
0.728643	-0.18593	0.000939
0.738693	-0.17588	0.000991

The best fit tuning parameters α and β are found after several runs of iterations. Those values are used to complete the equations because of eliminating the unknown variables.

Table 4.2 Best fit of tuning parameters

Vafaei Sefti et al	Hu et al
α= 0.3104753026	α = 0.4016292147
β = -0.570452451	β = -0.397226641
SSE = 0.0019135886	SSE = 1.24E-07

The results of prediction on amount of precipitated asphaltene can be clearly seen in table 4.3 and 4.4 for Vafaei Sefti et al and Hu et al, respectively. The predicted (model) and observed (experiment) values have a good agreement due to insignificant residual errors produced.

Table 4.3 Model vs Experimental data (Vafaei Sefti et al)

Mol% CO2 Injected	Mol% CO2 in Liquid	Wexp (Vafaie Sefti et al)	Wmodel	Residual Error
2.4942	4.039	0.789474	0.786032	0.00436
11.5012	10.146	4.52632	4.489363	0.008165
18.9838	14.271	7.05263	7.008497	0.006258
25.2194	17.177	8.68421	8.650574	0.003873
30.485	19.31	9.73684	9.713356	0.002412
35.0577	20.976	10.3684	10.34899	0.001872
40.0462	22.619	10.7895	10.74866	0.003785
42.5404	23.391	11.1053	11.07104	0.003085
46.0046	24.385	11.2632	11.21521	0.004261
48.77	25.136	11.3158	11.24836	0.00596

Table 4.4 Model vs Experimental data (Hu et al)

Mol% CO2 Injected	Mol% CO2 in Liquid	Wexp (Hu et al)	Wmodel	Residual Error
51.6	32.251	0.06	0.060234	-0.00389
63.8	35.875	0.23	0.230019	-8.3E-05
71.6	37.744	0.32	0.319771	0.000717
80.2	39.463	0.42	0.42013	-0.00031

4.1.2 Prediction of Precipitated Asphaltene due to Pressure Effects

The subsequent step is to generate profile of weight percent of precipitated asphaltene with various pressures. In this study, recombined oils with 2.494% and 51.6% mol of CO2 injected are taken from Vafaei Sefti et al and Hu et al, respectively.

In general for Vafaei Sefti et al case (shown in figure 4.2a), it is observed that there is no considerable difference on the amount of precipitated asphaltene for low temperature (T < 50 deg C) and high temperature (T > 100 deg C). On the contrary, an enormous amount of precipitation becomes visible ranging of temperature from 50 to 100 deg C. Within this temperature range, the precipitated asphaltene is more produced as pressure increases.

In figure 4.3a, it should be noted that at pressure of 130 bar, 140 bar and 150 bar, the corresponding boiling temperatures are 60.03 deg C, 78.33 deg C and 99.85 deg C, respectively. The maximum amount of precipitation is most likely formed near its saturation points (boiling temperatures) for each pressure profile.

Figure 4.3b also shows the similar tendencies that peak of precipitated asphaltene appear around saturation points.

In addition, Mansoori[41] reported the profile of asphaltene deposited from live oil which demonstrated the same trends, higher pressure produces more asphaltene deposits (figure 4.2).

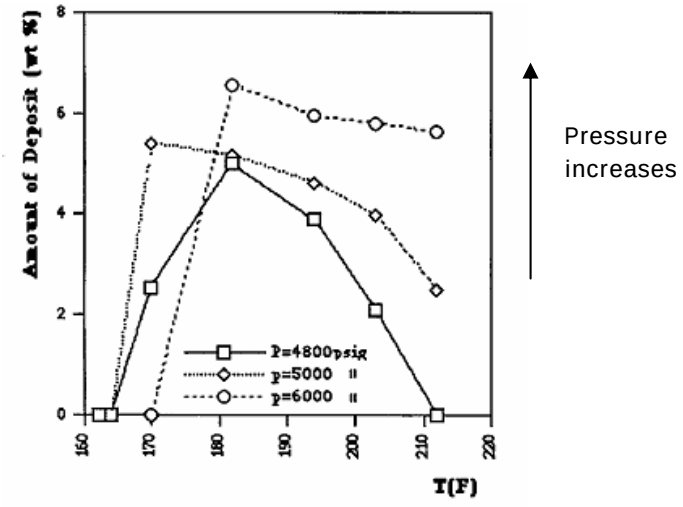

Figure 4.2 Trend of amount of asphaltene deposited as temperature and pressure change (taken from Mansoori[41])

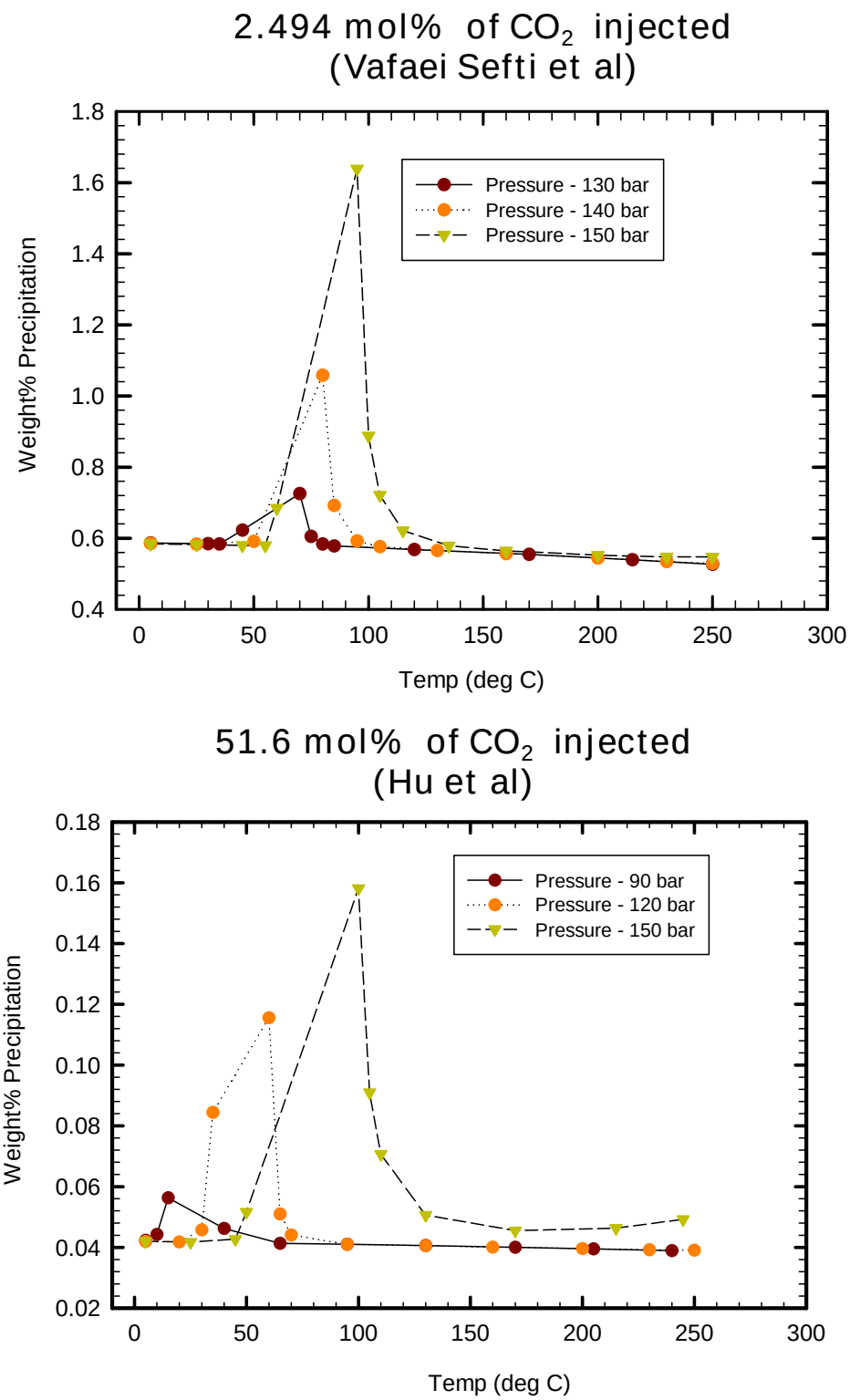

Figure 4.3 Prediction of precipitated asphaltene with a decrease in temperature at various pressures by using recombined oil from (a) 2.494mo%l CO_2 injected Vafaei Sefti et al (b) 51.6mol% CO_2 injected Hu et al

4.1.3 Prediction of Precipitated Asphaltene due to Temperature Effects

Recombined oils taken as study case are from Vafaei Sefti et al with 30.485 mol% CO2 injected and Hu et al with 63.8 mol% CO_2 injected.

The same scenario was applied to investigate temperature effects on asphaltene behavior. In this study, during depressurization the amount of precipitated asphaltene are estimated at different temperatures.

The profile of precipitation either for Vafaei Sefti et al or Hue et al (see in figure 4.5a and 4.5b, respectively) are exactly the same behavior as explained in the previous section during decreasing temperature condition, i.e. the higher temperature will produce more precipitated asphaltene.

Abundant precipitations are observed around bubblepoint pressures. For Vafaei Sefti et al, it is interesting to note that the corresponding bubblepoint pressures at temperature of 30 deg C, 60 deg C and 125 deg C are 95.73 bar, 120.96 bar and 164.94 bar, respectively.

Soulgani et al[I][42] performed a precipitation test during depressurization condition at different temperatures. The result of asphaltene precipitation measurement demonstrated a similar performance as predicted in this study, i.e an enormous precipitation will be produced at higher temperature (figure 4.4).

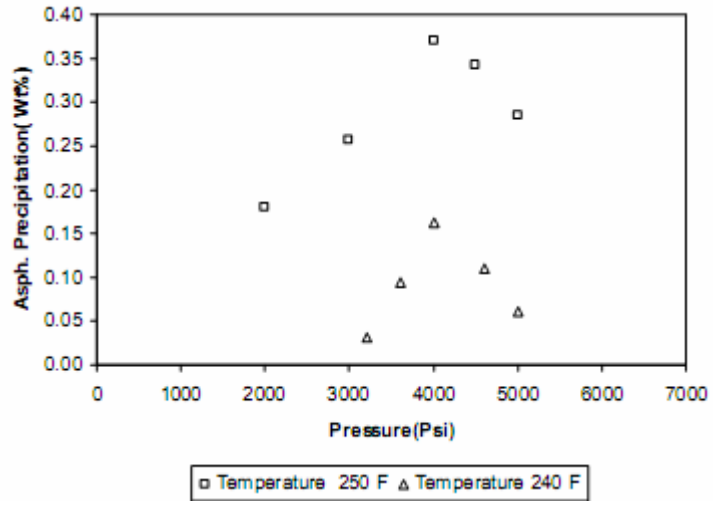

Figure 4.4 Result of asphaltene precipitation measurement by Soulgani et al[I][42] at different temperatures during depressurization process

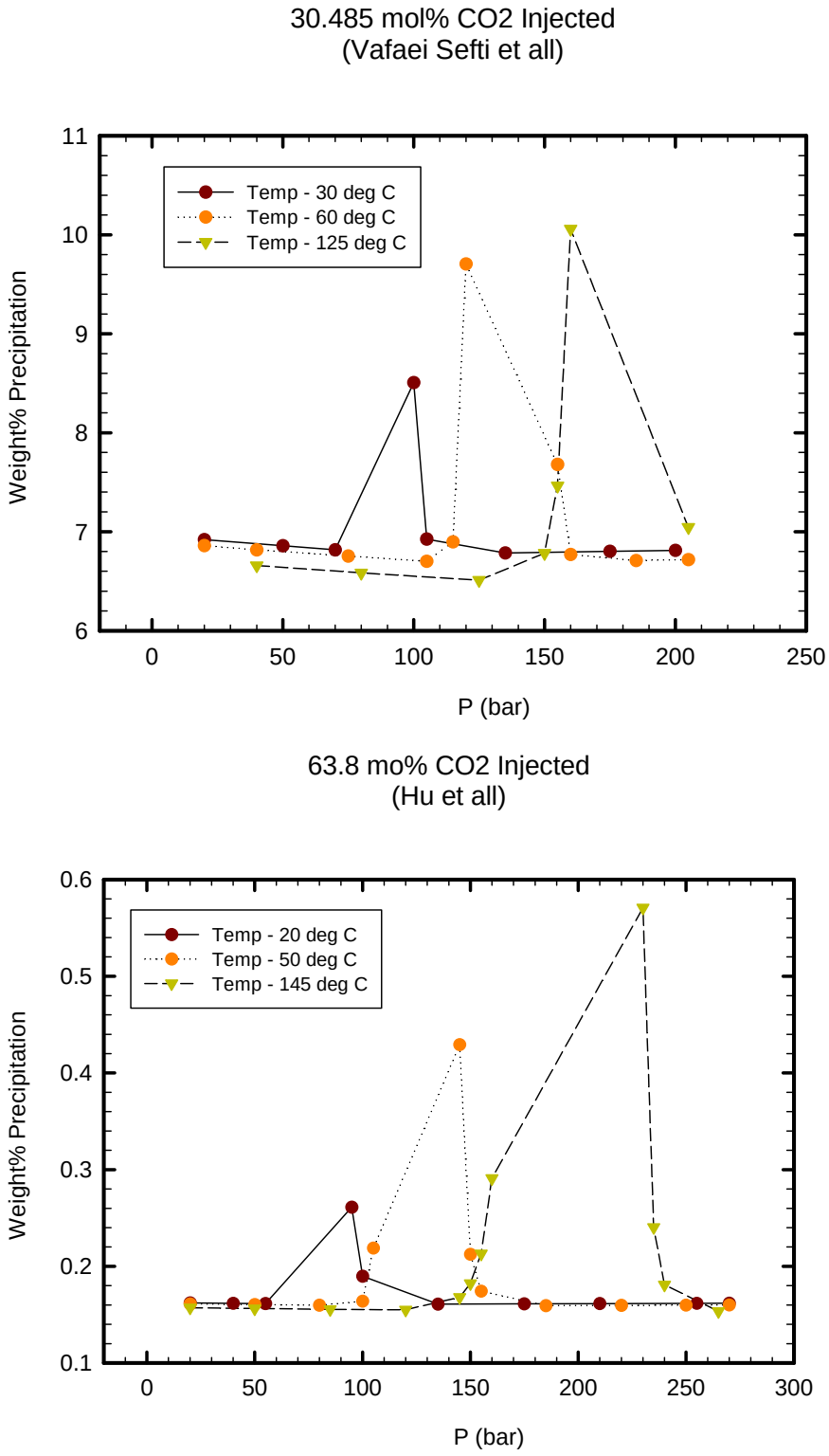

Figure 4.5 Prediction of precipitated asphaltene during depressurization at various temperatures by using recombined oil from (a) 30.485 mo%l CO_2 injected Vafaei Sefti et al (b) 63.8 mol% CO_2 injected Hu et al

It should be pointed out that temperature contributes more effects on precipitation compared to pressure, i.e. in stable

asphaltene region (outside of asphaltene precipitation envelope), marked by red dotted line in figure 4.6, the difference magnitude of precipitated asphaltene at different temperatures are much higher rather than pressures.

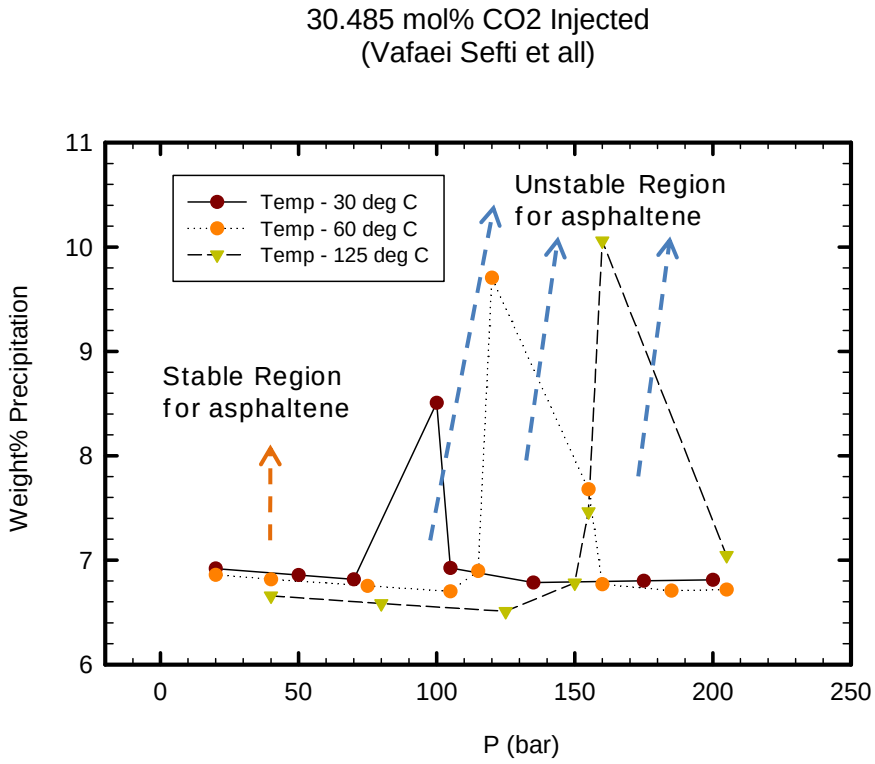

Figure 4.6 Illustration of unstable and stable regions for asphaltene at various temperatures during depressurization.

Asphaltene solubility is less dependent on pressure compared to temperature. An increase in temperature mainly affects the aggregation of asphaltene by reducing the power of the oil. This statement still becomes a debate in literatures. Some literatures stated that the aggregation of asphaltene decreases as temperature increases while others reported a reverse behavior that asphaltene precipitation increases with temperature[15].

From figure 4.6, in unstable region (inside of asphaltene precipitation envelope), higher temperature produces more precipitation due to asphaltene solubility is higher when the oil is heavier which indicates asphaltene tends to stay in the solution (oil)[15]. Moreover, figure 4.7 reported by Burke et al[5] that compares the solubility parameter of oil at different temperatures. It can be concluded that less precipitation produced at lower

temperature because the solubility parameter of oil increases as temperature decreases.

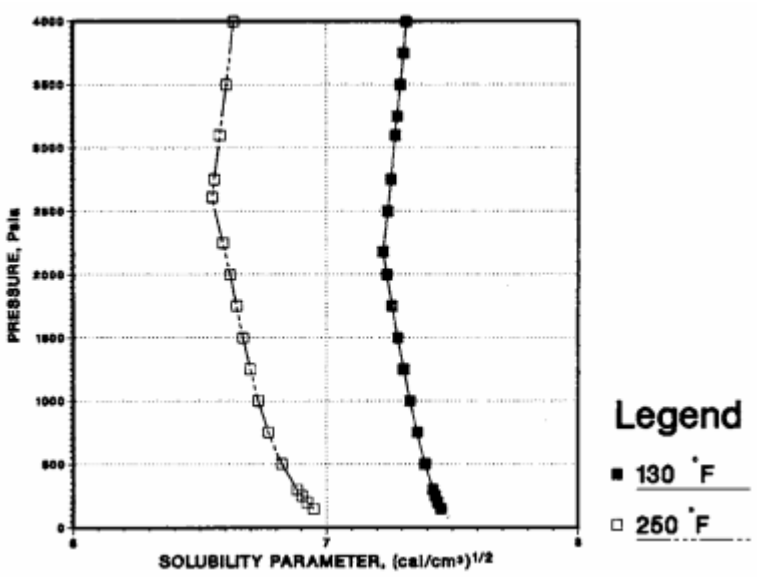

Figure 4.7 Relationship of solubility parameter and pressure at different temperatures[5]

4.1.4 Prediction of Precipitated Asphaltene due to CO_2 Injection Effects

A CO_2 injection is categorized as a miscible gas injection which has ability to mix and create one phase with oil by multiple contacts miscibility (known as MCM process). CO_2 decreases the interfacial tension (IFT) of oil so that CO_2 dissolves in oil. By adding more light components in oil, it improves capability of oil mobilization which gives a similar benefit like “gas lift”. On the other hands, an injection of CO_2 changes the composition and phase behavior of fluid. Changes in oil composition tend to induce asphaltene instability which triggers to asphaltene precipitation and deposition. It has been reported that CO_2 flooding can be favorable condition of asphaltene precipitation[3, 43].

For Vafaei Sefti et al case, data is taken at pressure of 100 bar while data taken from Hu et al at pressure of 120 bar.

Figure 4.8a presents three data sets of temperatures (i.e. 50, 100 and 180 deg C) with various mol % CO_2 injected. The precipitation seems increasing exponently as more mol% CO_2 injected for Vafaei et al while in figure 4.8b, the precipitation is linearly increasing as more injected of mol % CO_2.

Temperature has reverse effect as temperature increases. At low temperature to medium temperature (from 20 to 60 deg C), precipitation is less produced at 60 deg C. On the contrary, from medium to high temperature (keep increasing the temperature), from 60 to 90 deg C, precipitation of asphaltene is more pronounced. It should be noted that the corresponding saturation temperatures for Vafaei Sefti et al and Hu et al are 143.71 and 116.27 deg C, respectively. Theoretically, the precipitation of asphaltene reaches maximum amount at saturation temperature. For that reason, most likely production at temperature 90 deg C has been inside of unstable region of asphaltene which gives enormous precipitation as temperature increases.

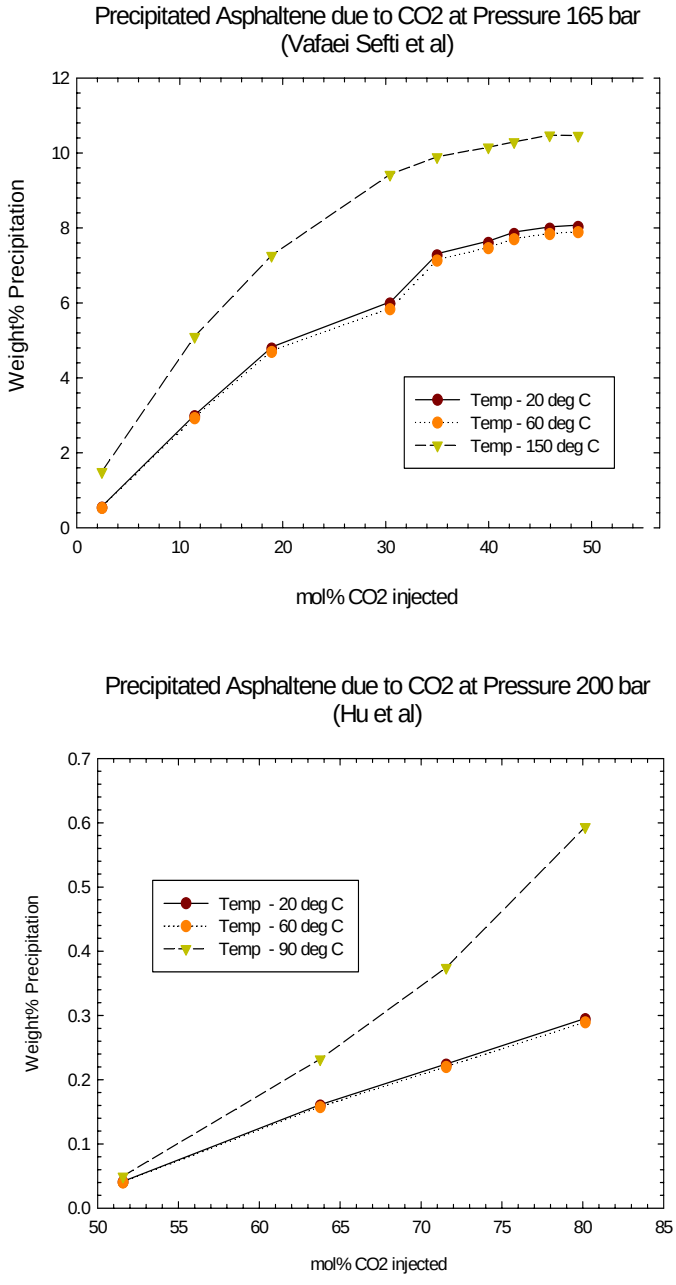

Figure 4.8 Precipitated asphaltene with various addition of mol% CO_2 injected and temperatures (a) at pressure 165 bar for Vafaei Sefti et al (b) at pressure 200 bar for Hu et al

4.2 Compositional Simulation for Water and CO_2 Flooding with Presence of Asphaltene Deposition at Different Temperatures

This section presents a simulation study on temperature effect with respect to asphaltene behavior. Temperature is a key variable on oil recovery performance. In general, as temperature increases, viscosity of oil is reduced so that oil phase becomes more mobile which improves the oil recovery. Meanwhile, as discussed earlier that higher temperature tends to stimulate precipitation of asphaltene and potentially produces deposit problems that can cause rigorous reduction on formation properties. Hence, sensitivities analysis in temperature is being main subject during simulation.

In addition, composition changes play an important role on oil recovery and asphaltene behavior as well. Water flooding is known as an immiscible displacement which has higher contact with oil rather than CO_2 flooding. CO_2 flooding creates a miscible zone at interface between oil and CO_2 by dissolving CO_2 in oil which can compensate the pressure drop during displacement. At the same time, the light constituents in oil might be extracted out from oil which make difficult on producing the residual oil. For that reason, different types of injected fluids (water and CO_2) are simulated in this study to address those concerns.

4.2.1 Oil Recovery Performance

Results of sensitivities analysis on temperature at 122F (50 deg C), 212F (100 deg C) and 392 F (200 deg C) and injected fluids (water and CO_2) to oil recovery are presented in figure 4.9.

For all temperatures, CO_2 recovers more oil than water due to higher sweep efficiency. The effect of temperature on CO_2 flooding is more pronounced compared to water flooding. For comparison (see figure 4.10 and 4.11), during water flooding the reduction of total oil recovery at 122 F and 392 F is still less than 1 MMSTB while during CO_2 flooding is approximately 1.5 MMSTB. Although the

effect of higher temperature on reducing the total oil recovery during CO_2 flooding injection of CO_2 is still more promising than water.

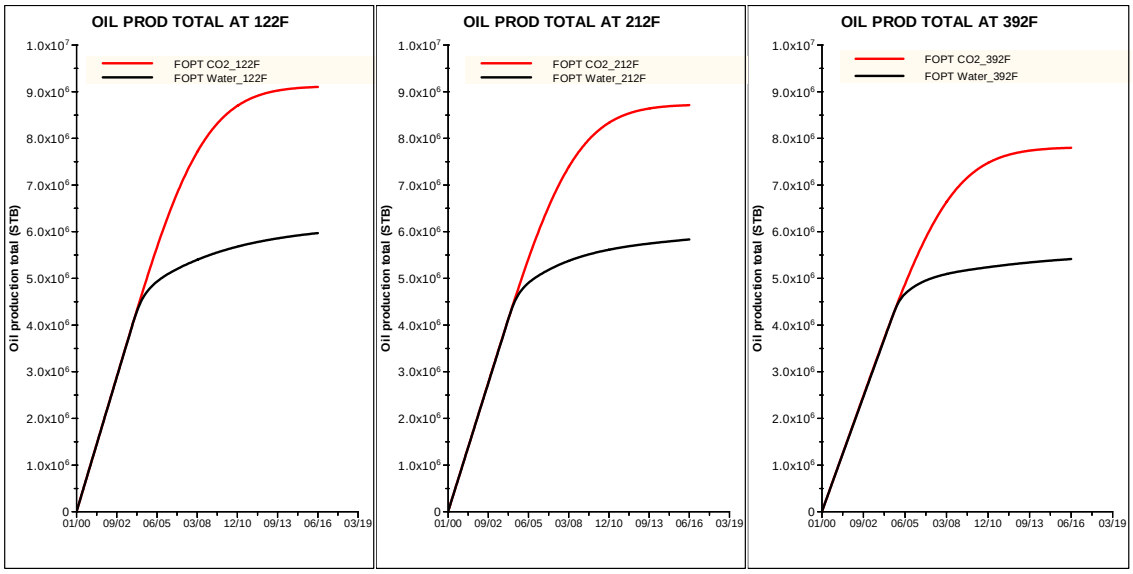

Figure 4.9 Total oil recovery by water and CO_2 at different reservoir temperatures 122 F, 212 F and 392 F

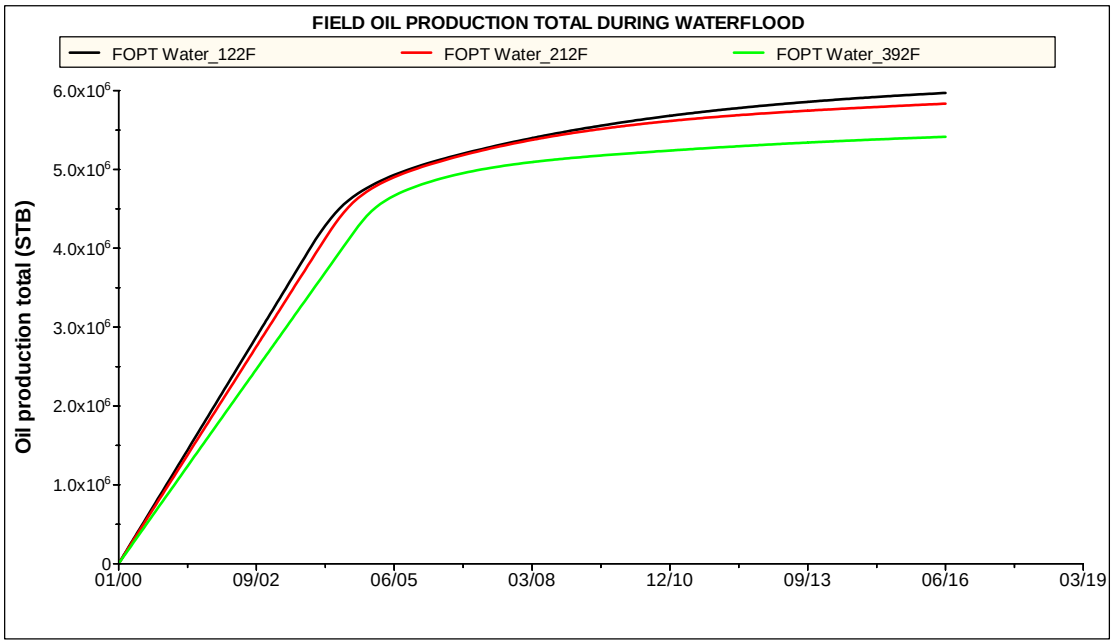

Figure 4.10 Total oil recovery during water flooding at various temperatures

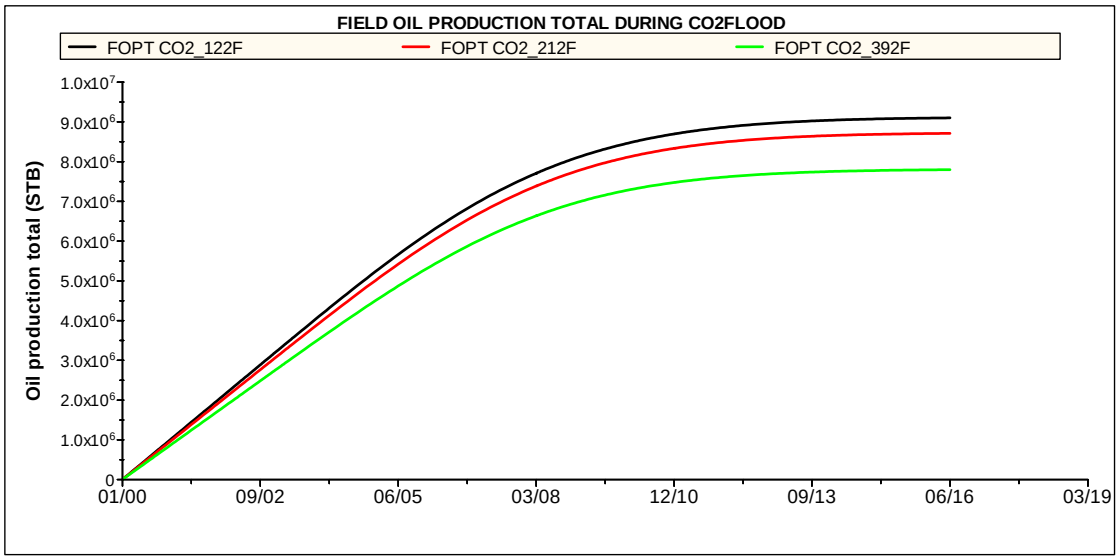

Figure 4.11 Total oil recovery during CO_2 flooding at various temperatures

It has been reported that the initial oil in place at surface condition is 11.238 MMSTB. Because of using a simulator ECLIPSE 300 (compositional model), a keyword for retrieving a recovery factor is unavailable so that by dividing the cumulative oil production with the initial oil in place, oil recovery factor can be estimated. Table 4.5 shows comparison of oil recovery factor attained by water and CO_2 injections. CO_2 injection has a tremendous effect at lower temperature (122 F) on lowering the residual oil saturation.

Table 4.5 Oil recovery factor at various reservoir temperatures during water flooding and CO_2 flooding

Temp (F)	Recovery Factor (Water Flooding)	Recovery Factor (CO_2 Flooding)
122	53.11%	80.97%
212	51.90%	77.50%
392	48.16%	69.37%

Higher sweep efficiency during CO_2 flooding can be explained by comparing oil production rates between water and CO_2 flooding. In the beginning, the oil production rates during water and CO_2 flooding are similar, since in the end of 2003 a sharp drop in oil productivity observed during water flooding. During CO_2 flooding, a gradual declining in oil production rates which gives more oil produced (see figure 4.12).

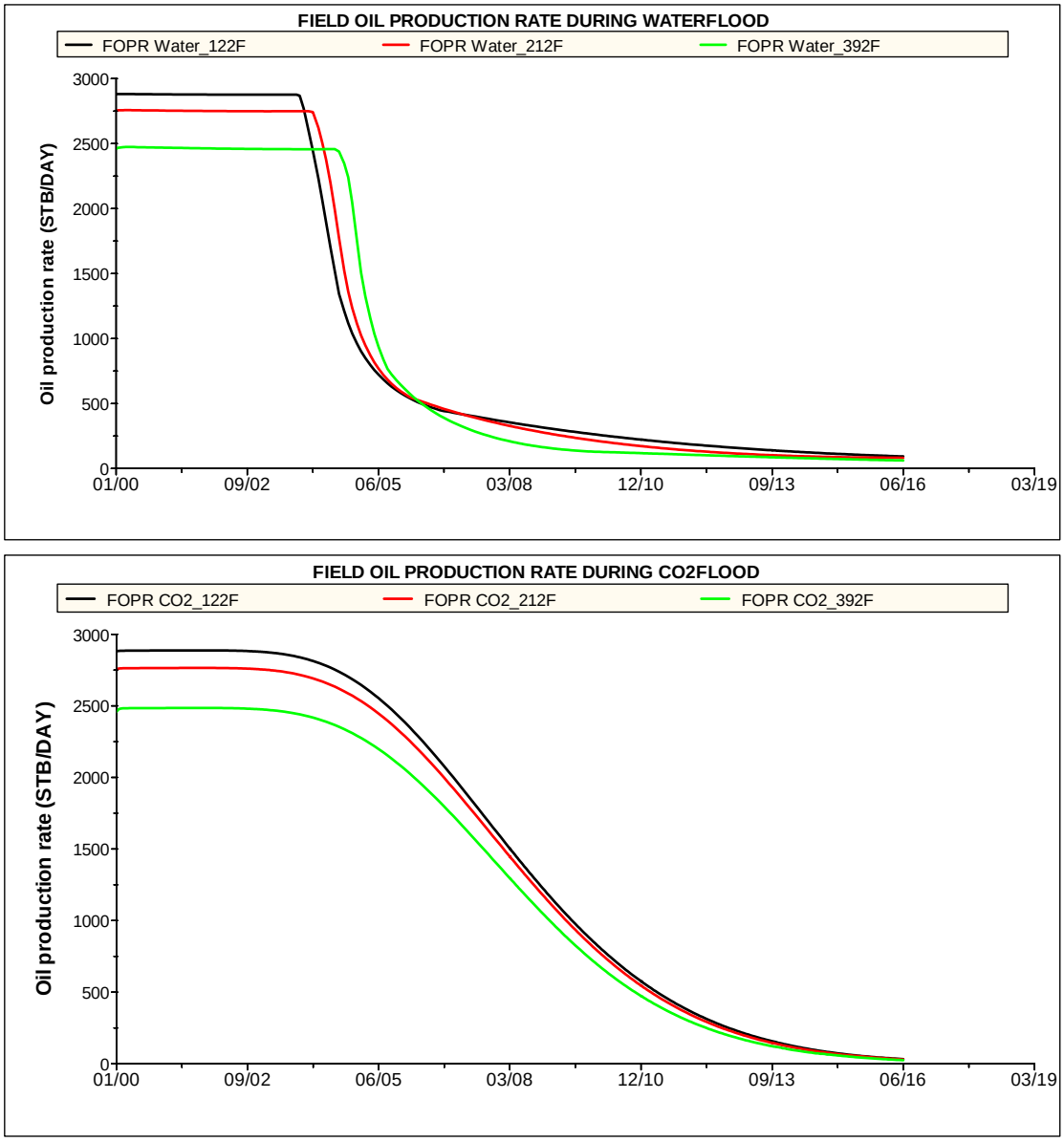

Figure 4.12 Oil production rates during water and CO_2 flooding at different temperatures

Figure 4.13 presents the reservoir pressure for both water and CO2 flooding that probably can enlighten the occurrence of a sudden decline of oil rates during water flooding. It seems that the influence of pressure support by water flooding in the reservoir takes more time compared to CO_2 flooding. CO_2 injection gives pressure support to the reservoir so that drawdown due to CO_2 injection is much higher than water injection.

Water is immiscible with oil which has better contact with oil. It does not warranty for higher oil recovery. During water flooding, it can be clearly seen that a massive pressure drop appears in 2002.

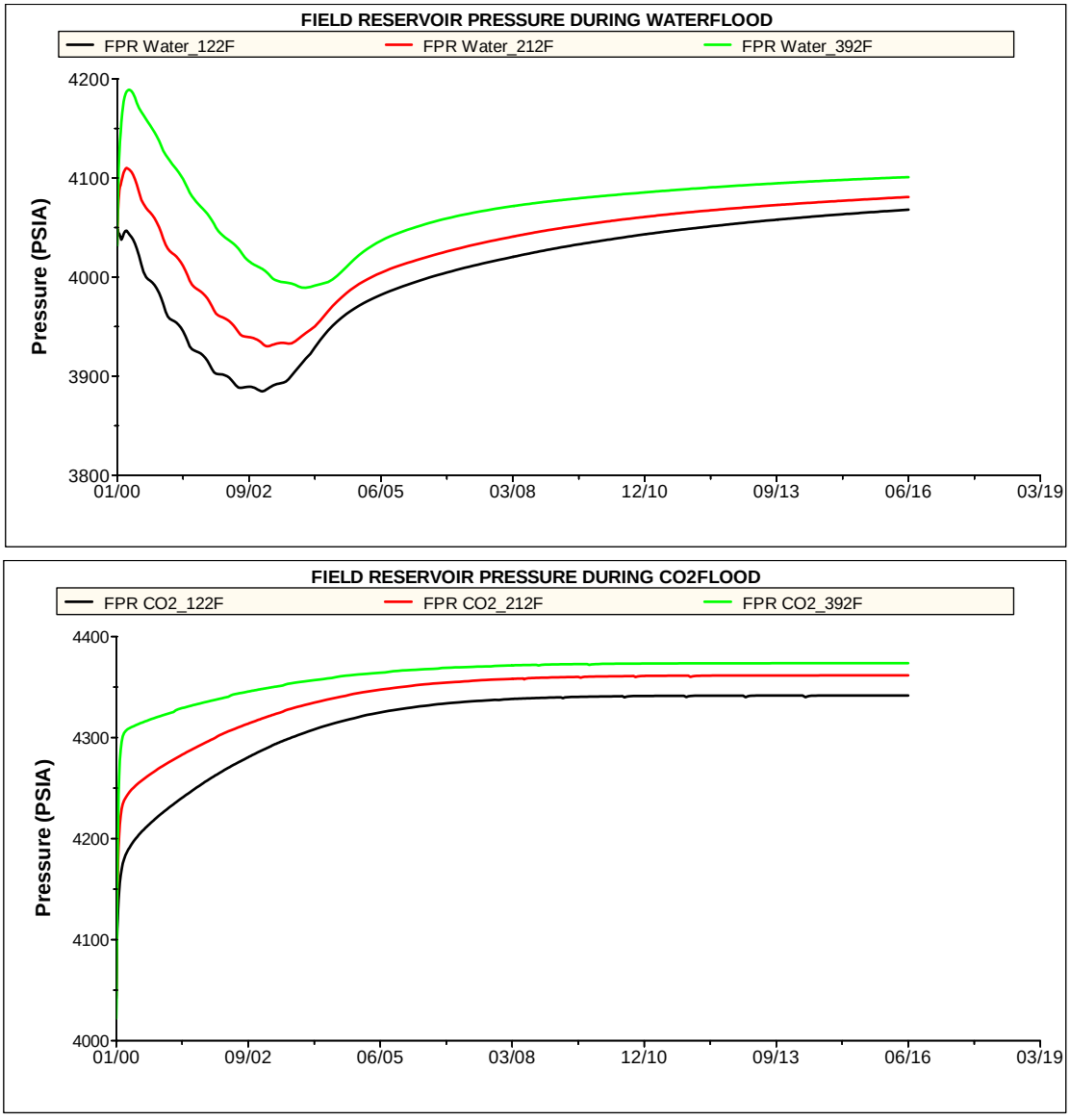

Figure 4.13 Reservoir pressure during water and CO_2 flooding at different temperatures

4.2.2 Displacement Performance

To study displacement process by water and CO_2 injection, the following figures visualize the distribution of oil saturation at different temperatures and production times.

As reported previously, the initial oil saturation is 0.84. It is meaningful to have a clear picture how the distribution of oil saturation during injection and post injection period. The Distribution of oil at temperature 122 F, 212 F and 392 F are given in figure 4.14, 4.15 and 4.16, respectively.

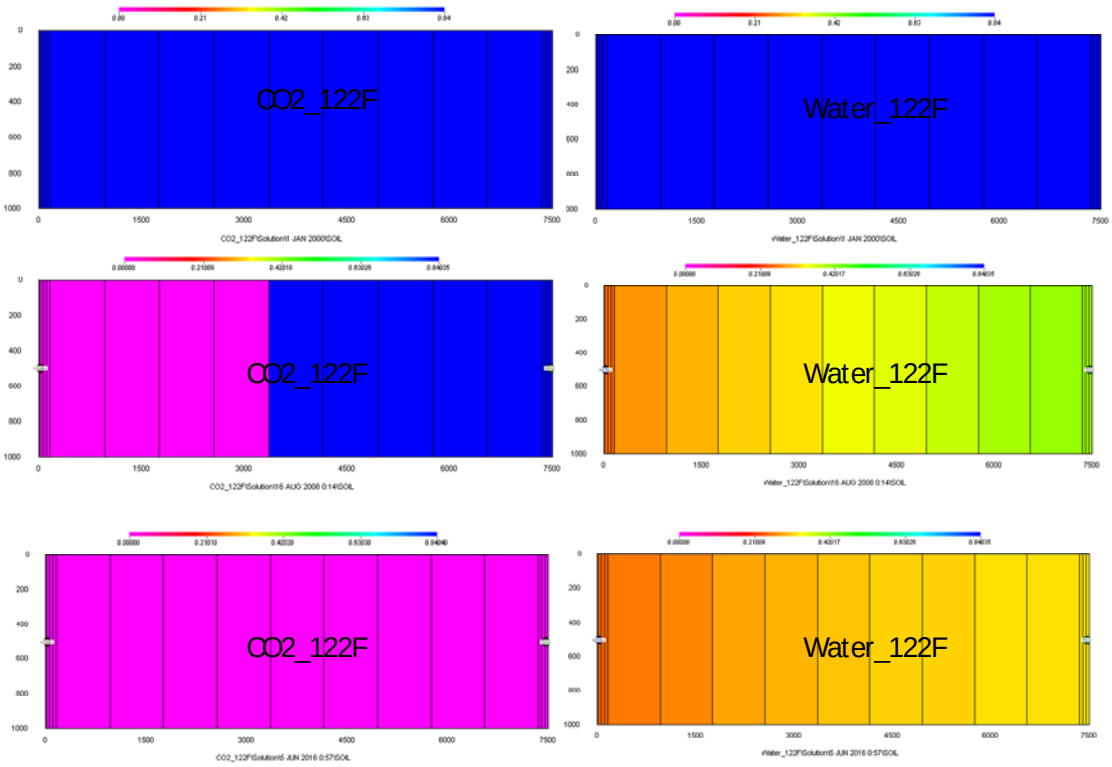

Figure 4.14 Oil saturation distribution during injection and post injection of water and CO_2 at temperature of 122 F

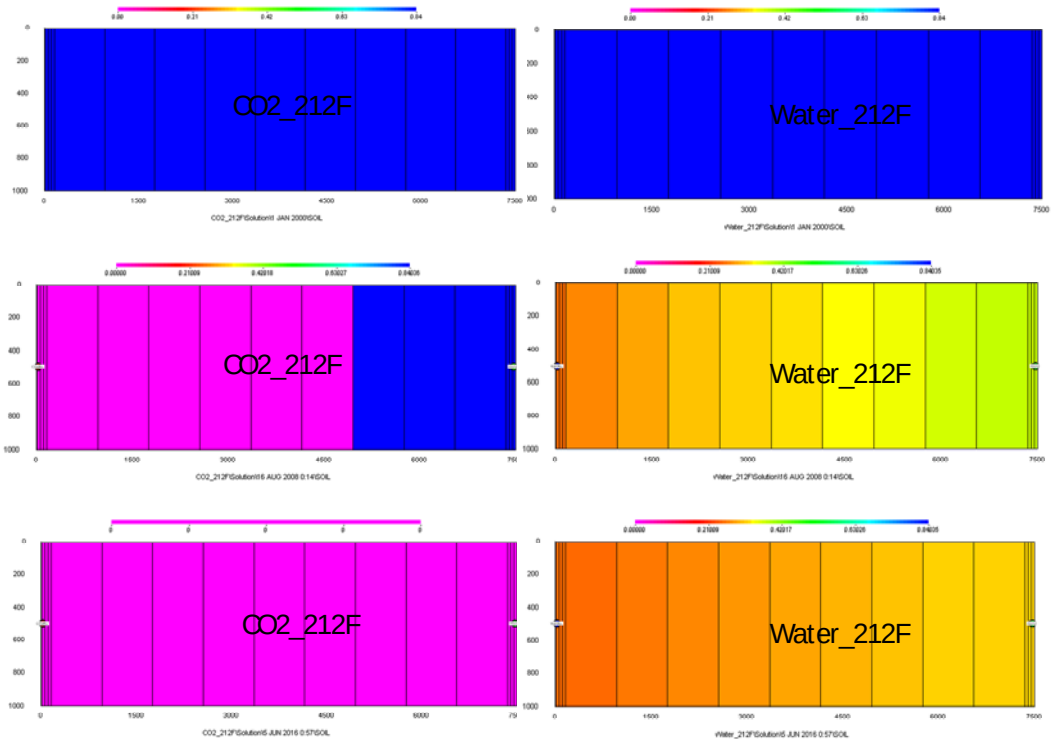

Figure 4.15 Oil saturation distribution during injection and post injection of water and CO_2 at temperature of 212 F

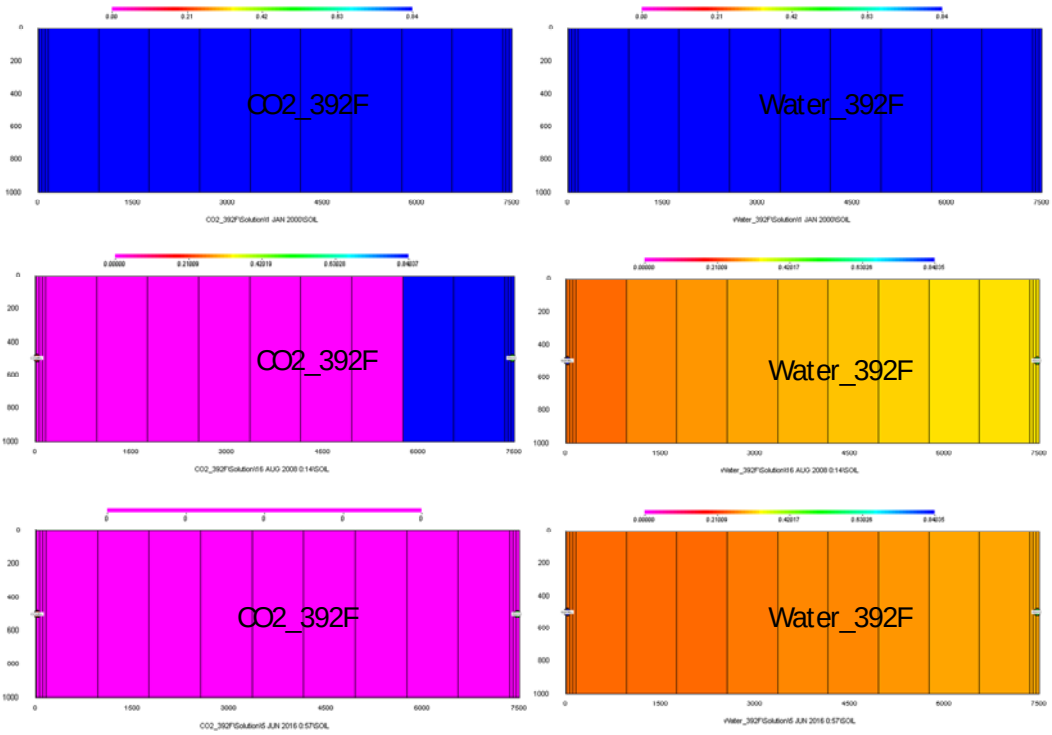

Figure 4.16 Oil saturation distribution during injection and post injection of water and CO_2 at temperature of 392 F

During displacement process, the displacement front by CO_2 is very obviously noticeable (“piston-like” displacement) indicating higher sweep efficiency. Unlikely CO_2 flooding, the distribution of oil saturation during water flooding is a continuous which proves that oil has not been swept entirely by water, there are still many residual oil left in the reservoir.

At higher temperature during CO_2 and water flooding, the displacement front moves slightly forward compared to the lower temperature which points out that sweep efficiency is higher at higher temperature. This is contradictive statement as mentioned earlier that lower oil recovery attained at higher temperature. The explanation of such inconsistent behavior will be emphasized further details in the following section.

4.2.3 Deposition of Asphaltene

During production and injection with different fluids types, the ongoing process of oil recovery occurs in dynamic conditions, i.e. changes in pressure, temperature and oil composition, which can affect to asphaltene behavior.

The concept of investigation in this study is to compare the amount of asphaltene volume fraction net deposit at production and injection points which both points are having much exposure with fluids. Figure 4.17, 4.18 and 4.19 compare the asphaltene volume fraction net deposit during water and CO_2 flooding at temperature 122 F, 212 F and 392 F, respectively.

At injection point during CO_2 flooding, no asphaltene deposition appears while during water flooding more injection of water will produce more deposition of asphaltene. On the other sides, at production point, water flooding has more asphaltene deposition than CO_2 flooding although they have an identical rate of deposition in the beginning of production.

For different temperature conditions, at higher temperature, asphaltene volume fraction net deposit is higher than at lower temperature. It confirms why at higher temperature the sweep efficiency is slightly better but lower in oil recovery because of higher amount of asphaltene deposition.

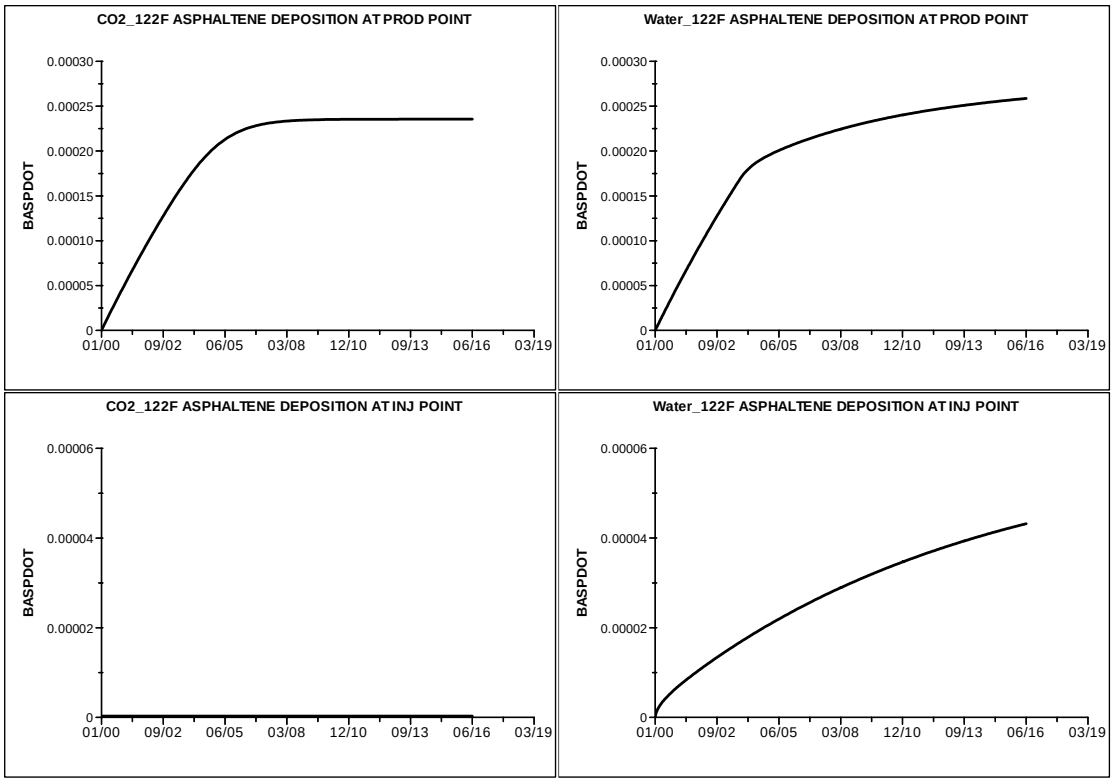

Figure 4.17 Asphaltene volume fraction net deposit at production and injection points during CO_2 flooding and water flooding at temperature of 122 F

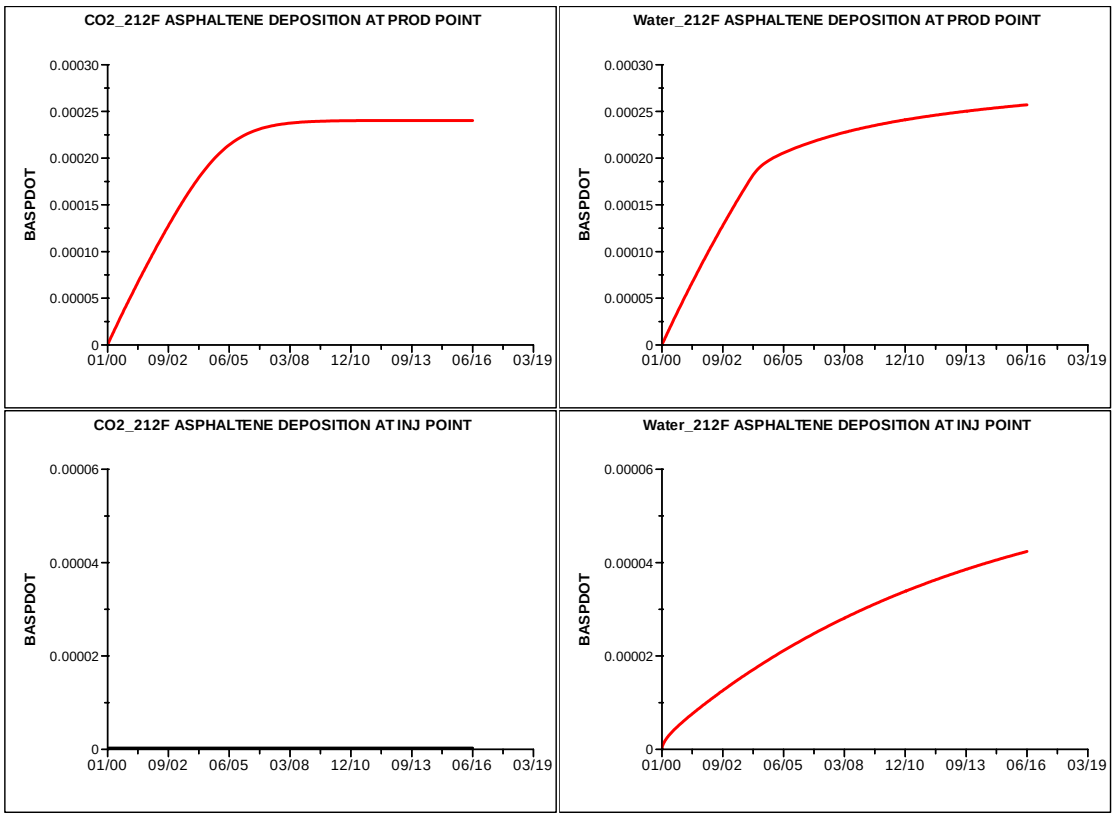

Figure 4.18 Asphaltene volume fraction net deposit at production and injection points during CO_2 flooding and water flooding at temperature of 212 F

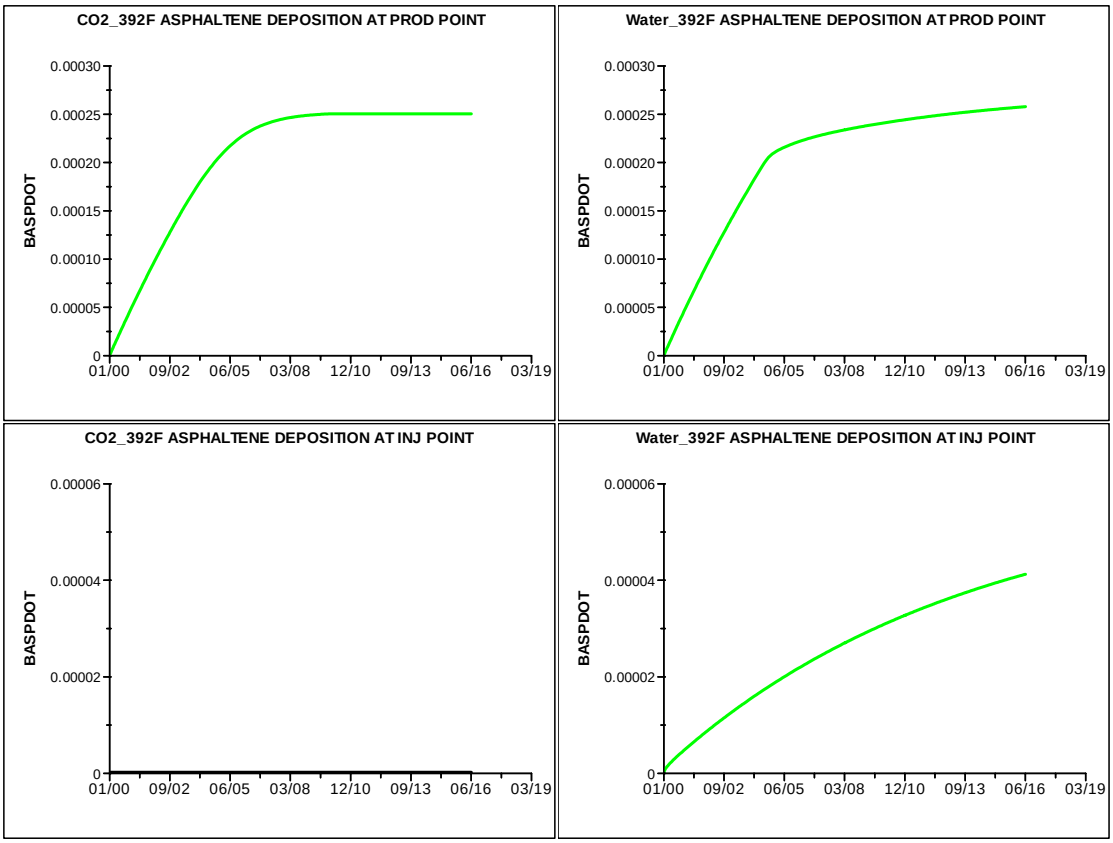

Figure 4.19 Asphaltene volume fraction net deposit at production and injection points during CO_2 flooding and water flooding at temperature of 392 F

Asphaltene deposition is abundant at production point as shown in figure 4.20.

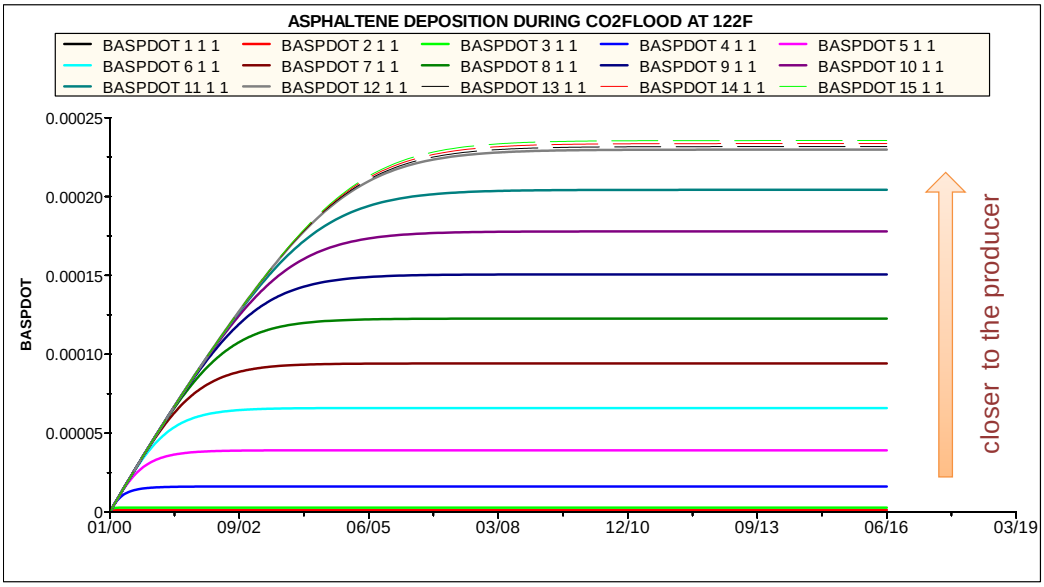

Figure 4.20 – Distribution of asphaltene volume fraction net deposit

4.2.4 Permeability Damage

As deposition of asphaltene encountered during production and injection, the formation properties is potentially reduced because of reduced effective mobility for oil which is caused by several reasons such as blocking pore throats, wettability alteration and increasing the oil viscosity. In this section, it highlights the permeability damage (reduction multiplier) which can be symbolized by the ratio of actual permeability affected by asphaltene deposition over initial permeability (K / K_i).

At injection point during CO_2 flooding, no permeability damage encountered as no deposition of asphaltene appears, while during water flooding, due to increasing of asphaltene deposition the permeability reduction is gradually rising.

Typically, permeability reduction during water flooding at production point is continuously increasing whereas during CO_2 flooding at certain period of times permeability reduction does not arise anymore (steady) with time.

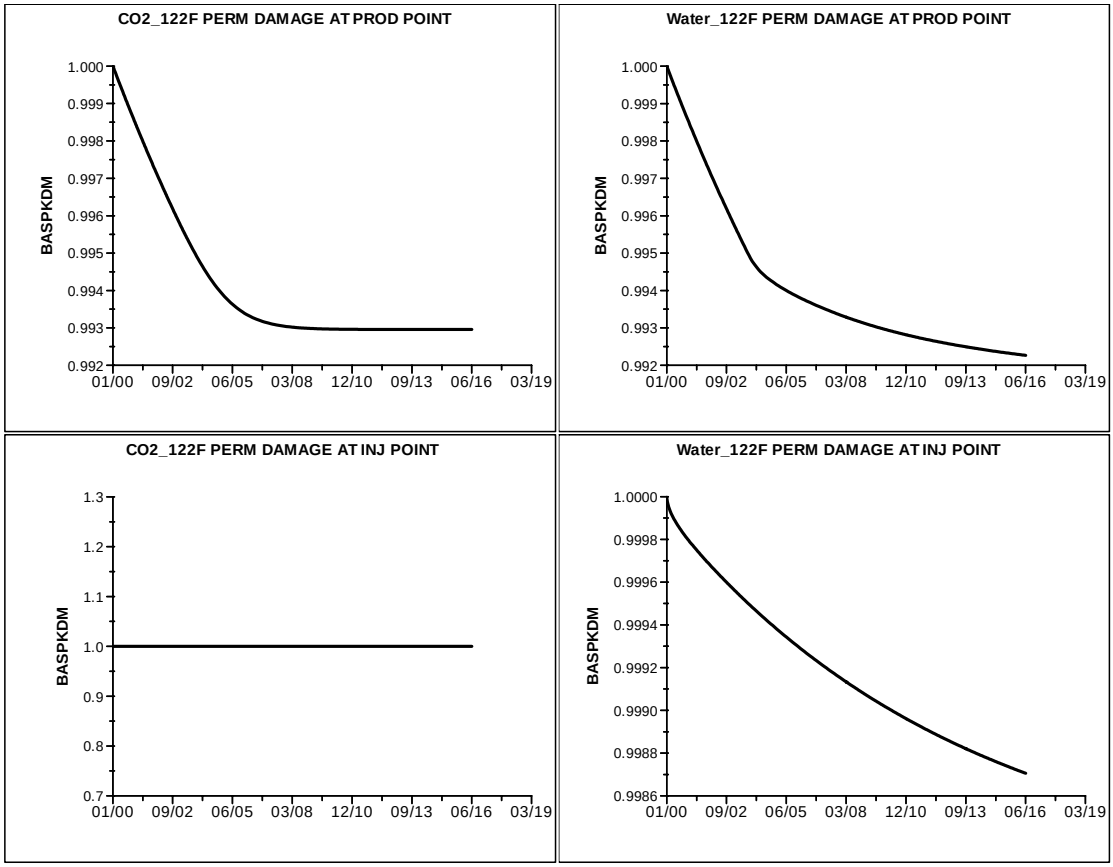

Figure 4.21 Permeability reduction at injection and production points during CO_2 and water flooding at temperature of 122 F

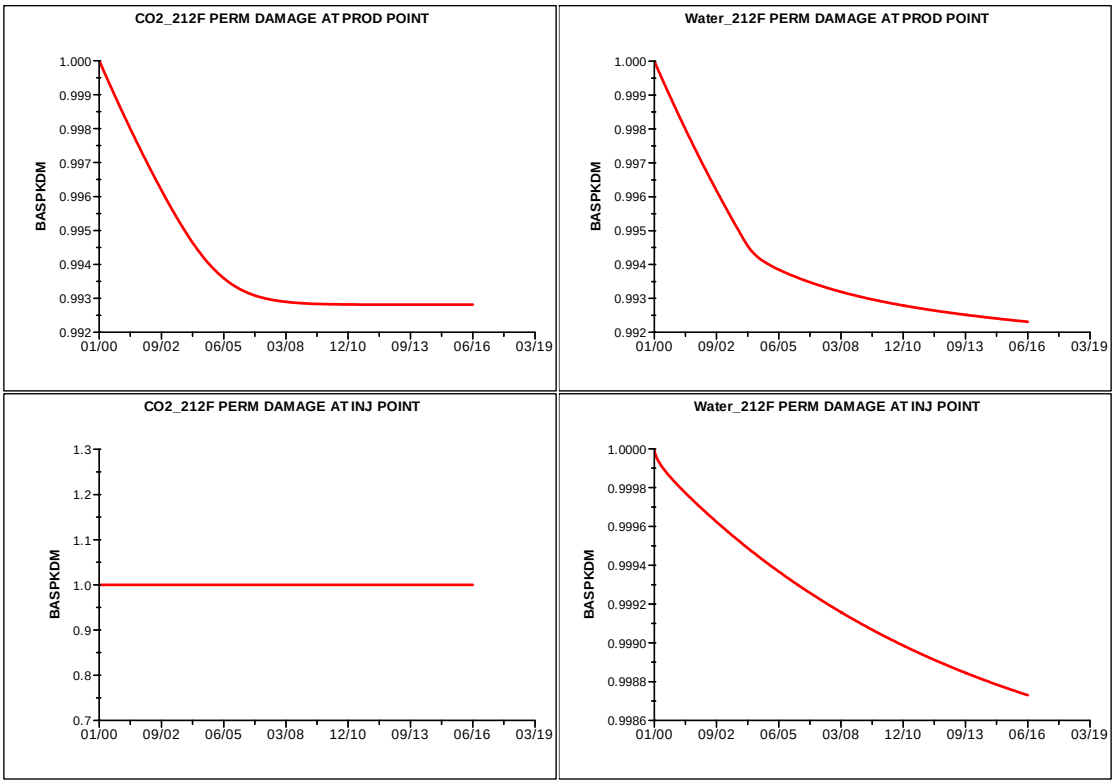

Figure 4.22 Permeability reduction at injection and production points during CO_2 and water flooding at temperature of 212 F

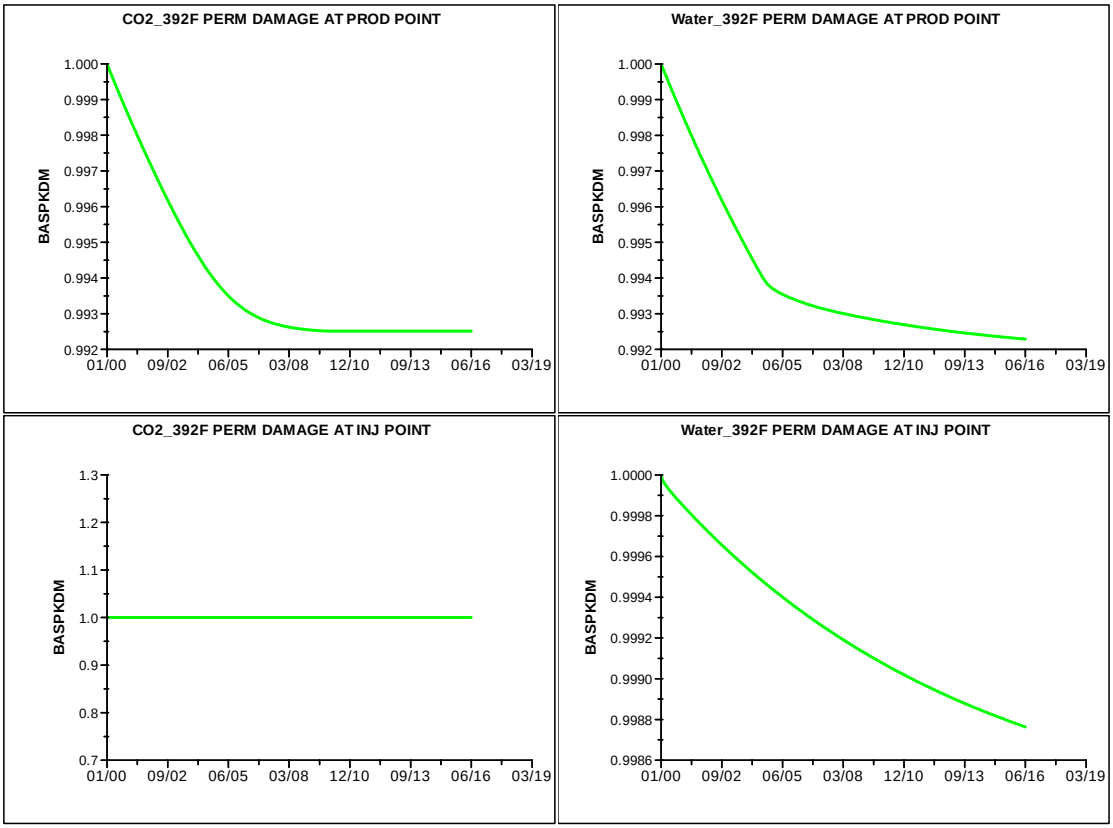

Figure 4.23 Permeability reduction at injection and production points during CO_2 and water flooding at temperature of 392 F

Basically, the permeability reduction follows the same trend of asphaltene deposition because the damage itself is caused by deposition. At higher temperature, deposition of asphaltene is slightly higher compared to at lower temperature. As a result, reduction in permeability is more pronounced at higher temperature.

The same distribution of permeability reduction is shown in figure 4.24 as well as deposition of asphaltene, which is at production point the extra damage in permeability is observed.

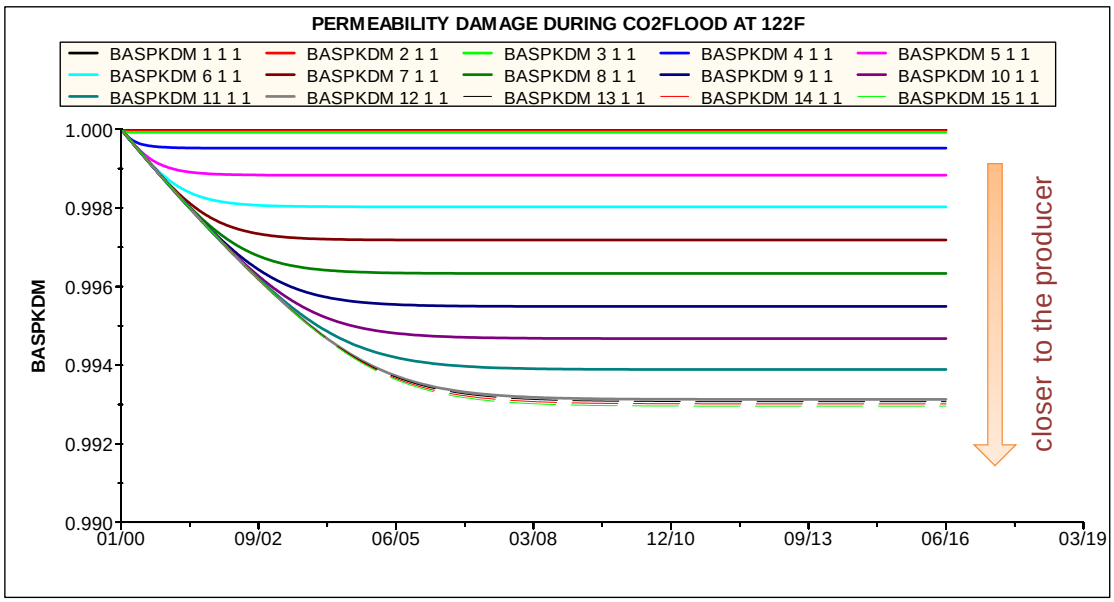

Figure 4.24 Distribution of permeability reduction during CO_2 flooding

CHAPTER 5 CONCLUSIONS AND FUTURE WORK

5.1 Conclusions

From this study, the following conclusions can be drawn:

1. An equation which is based on Flory-Huggins polymer-solution theory and Hildebrand solubility concept has been developed for modeling asphaltene precipitation.

2. The predictions show good agreements with the experimental results on the basis of experiment conditions (at specific pressure and temperature). The model is then possible to generate prediction of precipitated asphaltene at wide range of conditions to address various aspects which lead to asphaltene precipitation.

3. To validate the model, an iterative manner is applied to seek best fit tuning parameters required α and β. Process of fine-tuning the model is very crucial step which can greatly influence the accuracy of model.

4. Results of Prediction have confirmed from physics point of view (theory) that as pressure decreases (at above bubblepoint pressure), the asphaltene content in oil will decrease (amount of precipitated asphaltene increases) and only amount of least soluble content of asphaltene will remain in oil at bubblepoint pressure. In decreasing pressure (at below bubblepoint pressure) the asphaltene redissolves back into oil (amount of precipitated asphaltene decreases).

5. Outcomes generated by the model can be used to identify operating conditions which are favorable to asphaltene precipitation. This information is useful to be used in designing production strategies and EOR projects (CO_2 injection).

6. A compositional simulation is initiated with a simple reservoir model (1D horizontal reservoir) to cope dynamic conditions (pressure, temperature and composition changes) on asphaltene behavior.

7. Deposition of asphaltene is more pronounced during water flooding compared CO_2 flooding.

8. There is no asphaltene deposition present at injection point during CO_2 flooding.

9. The abundant deposition of asphaltene presents in the near producing well during water and CO_2 flooding.

10. It should be noted that temperature is hardly sensitive factor and occasionally temperature has a reverse effect from normal convention. It is interesting to examine temperature effect during CO_2 flooding. Normally for non-asphaltenic oil, viscosity of oil decreases as temperature increase which brings to higher oil recovery than at lower temperature. However, for asphaltenic oil with addition of CO_2, as temperature increases, oil recovery is smaller than at lower temperature because higher temperature reduces the solubility parameter of oil (more presence of deposition of asphaltene in the reservoir).

11. Simulation study shows that asphaltene deposition moves along the displacement front. It is because deposition is related with the development of miscibility for CO_2 flooding whereas during water flooding a gradual distribution of asphaltene deposition has been observed.

5.2 Future Works

There are very rarely found in literature (none) for available experimental data measured at different pressures and temperatures to study effect of CO2 injection with respects to asphaltene precipitation. Most of them reported measurement of precipitated asphaltene with various injection of CO2 concentration at fixed pressure and temperature.

For simulation study, it is highly recommended to use a 3D reservoir model which is more realistic than 1-D model. This proposed reservoir model probably exhibits full asphaltene behavior in order to complete the findings in this study and reveal the unexplained performance.

REFERENCES

1. Mullins, O.C., et al., *Asphaltenes, Heavy Oils, and Petroleomics*. 2007, New York, NY: Springer.
2. Shah Kabir, O.C., Mullins et al, *Asphaltenes - Problematic but Rich in Potential* in *Oilfield Review Summer 2007*. 2007, Schlumberger.
3. Kokal, S.L. and S.G. Sayegh, *Asphaltenes: The Cholesterol of Petroleum*, in *Middle East Oil Show*. 1995, 1995 Copyright 1995, Society of Petroleum Engineers, Inc.: Bahrain.
4. Fargas, F.M., Walter G, Chapman. *Modeling Asphaltene Phase Behavior In Crude Oil systems*. 2009 2010]; Slides of Presentation]. Available from: http://www.owlnet.rice.edu/~gjh/Consortium/Manuscripts/Asphaltene_Modeling_09.pdf.
5. Burke, N.E., R.E. Hobbs, and S.F. Kashou, *Measurement and Modeling of Asphaltene Precipitation (includes associated paper 23831).* SPE Journal of Petroleum Technology, 1990. **42**(11): p. 1440-1446.
6. MacMillan, D.J., et al., *A Unified Approach to Asphaltene Precipitation: Laboratory Measurement and Modeling.* SPE Journal of Petroleum Technology, 1995. **47**(9): p. 788-793.
7. Nghiem, L.X., et al., *Efficient Modelling of Asphaltene Precipitation*, in *SPE Annual Technical Conference and Exhibition*. 1993, 1993 Copyright 1993, Society of Petroleum Engineers, Inc.: Houston, Texas.
8. Pedersen, K.S. and C. Hasdbjerg, *PC-SAFT Equation of State Applied to Petroleum Reservoir Fluids*, in *SPE Annual Technical Conference and Exhibition*. 2007, Society of Petroleum Engineers: Anaheim, California, U.S.A.
9. Leontaritis, K.J. and G.A. Mansoori, *Asphaltene Flocculation During Oil Production and Processing: A Thermodynamic Collodial Model*, in *SPE International Symposium on Oilfield Chemistry*. 1987, 1987 Copyright 1987 Society of Petroleum Engineers, Inc.: San Antonio, Texas.
10. Victorotov, A.I. and A. Firoozabadi, *Thermodynamics of Asphaltene Precipitation in Petroleum Fluids by a Micellization Models.* AIChE Journal, 1996. **42**: p. 1753.
11. Hirschberg, A., et al., *Influence of Temperature and Pressure on Asphaltene Flocculation.* 1984. **24**(3): p. 283-293.
12. Hammami, A., et al., *Asphaltene Precipitation from Live Oils:â€‰ An Experimental Investigation of Onset Conditions and Reversibility.* Energy & Fuels, 1999. **14**(1): p. 14-18.
13. Parra-Ramirez, M., B. Peterson, and M.D. Deo, *Comparison of First and Multiple Contact Carbon Dioxide Induced Asphaltene Precipitation*, in *SPE International Symposium on Oilfield Chemistry*. 2001, Copyright 2001, Society of Petroleum Engineers Inc.: Houston, Texas.
14. Yen, T.F. and G.V. Chilingarian, *Asphaltenes and asphalts*. 1994, Amsterdam: Elsevier. b.
15. Ahmed, T., *Equations of state and PVT analysis: applications for improved reservoir modeling*. 2007, Houston, Tex.: Gulf Publ. XI, 553 s.
16. Hamouda, A.A., E.A. Chukwudeme, and D. Mirza, *Investigating the Effect of CO2 Flooding on Asphaltenic Oil Recovery and Reservoir Wettability.* Energy & Fuels, 2009. **23**(2): p. 1118-1127.
17. Wang, J.X., K.R. Brower, and J.S. Buckley, *Advances in Observation of Asphaltene Destabilization*, in *SPE International Symposium on Oilfield Chemistry*. 1999, Society of Petroleum Engineers: Houston, Texas.
18. Ratulowski, J., et al., *Flow Assurance and Subsea Productivity: Closing the Loop with Connectivity and Measurements*, in *SPE Annual Technical Conference and Exhibition*. 2004, Society of Petroleum Engineers: Houston, Texas.
19. Kawanaka, S., et al., *Thermodynamic and Colloidal Models of Asphaltene Flocculation*, in *Oil-Field Chemistry*. 1989, American Chemical Society: Washington, DC. p. 443-458.
20. Mei, H.Y., *Ph.D Thesis - The Precipitation Mechanism and Thermodynamic Model Research of Organic Solid*. 2000, U of Science and Technology of China.

21. Andersen, S.I. and J.G. Speight, *PETROLEUM RESINS: SEPARATION, CHARACTER, AND ROLE IN PETROLEUM.* Petroleum Science and Technology, 2001. **19**(1): p. 1 - 34.
22. Al-Kafeef, S.F., F. Al-Medhadi, and A.D. Al-Shammari, *A Simplified Method to Predict and Prevent Asphaltene Deposition in Oilwell Tubings: Field Case.* SPE Production & Operations, 2005. **20**(2): p. pp. 126-132.
23. Escobedo, J. and G.A. Mansoori, *Asphaltene and Other Heavy-Organic Particle Deposition During Transfer and Production Operations*, in *SPE Annual Technical Conference and Exhibition*. 1995, 1995 Copyright 1995, Society of Petroleum Engineers, Inc.: Dallas, Texas.
24. Leontaritis, K.J., *Asphaltene Near-wellbore Formation Damage Modeling*, in *SPE Formation Damage Control Conference*. 1998, 1998 Copyright 1998, Society of Petroleum Engineers, Inc.: Lafayette, Louisiana.
25. alizadeh, n., et al., *Simulating the Permeability Reduction due to Asphaltene Deposition in Porous Media*, in *International Petroleum Technology Conference*. 2009, 2009, International Petroleum Technology Conference: Doha, Qatar.
26. Kim, S.T., M.-E. Boudh-Hir, and G.A. Mansoori, *The Role of Asphaltene in Wettability Reversal*, in *SPE Annual Technical Conference and Exhibition*. 1990, 1990 Copyright 1990, Society of Petroleum Engineer Inc.: New Orleans, Louisiana.
27. Boer, R.B.d. and K. Leerlooyer, *Screening of Crude Oils for Asphalt Precipitation*, in *SPE European Petroleum Conference*. November 1992, SPE: Cannes, France.
28. Jamaluddin, A.K.M., et al., *Laboratory Techniques to Measure Thermodynamic Asphaltene Instability.* 2002. **41**(7).
29. Yen, A., Y.R. Yin, and S. Asomaning, *Evaluating Asphaltene Inhibitors: Laboratory Tests and Field Studies*, in *SPE International Symposium on Oilfield Chemistry*. 2001, Copyright 2001, Society of Petroleum Engineers Inc.: Houston, Texas.
30. Flory, P.J., *Thermodynamics of High Polymer Solutions.* The Journal of Chemical Physics, 1942. **10**(1): p. 51-61.
31. Kawanaka, S., S.J. Park, and G.A. Mansoori, *Organic Deposition From Reservoir Fluids: A Thermodynamic Predictive Technique.* SPE Reservoir Engineering, 1991. **6**(2): p. 185-192.
32. Cimino, R., et al., *Thermodynamic Modelling for Prediction of Asphaltene Deposition in Live Oils*, in *SPE International Symposium on Oilfield Chemistry*. 1995, 1995 Copyright 1995, Society of Petroleum Engineers, Inc.: San Antonio, Texas.
33. Novosad, Z. and T.G. Costain, *Experimental and Modeling Studies of Asphaltene Equilibria for a Reservoir Under CO2 Injection*, in *SPE Annual Technical Conference and Exhibition*. 1990, 1990 Copyright 1990, Society of Petroleum Engineers Inc.: New Orleans, Louisiana.
34. Kokal, S.L., et al., *Measurement And Correlation Of Asphaltene Precipitation From Heavy Oils By Gas Injection.* 1992. **31**(4).
35. Chung, F., P. Sarathi, and R. Jones, *"Modeling of Asphaltene and Wax Precipitation" Topical Report in NIPER-498.* DOE, January 1991.
36. Chapman, W.G., et al., *SAFT: Equation-of-state solution model for associating fluids.* Fluid Phase Equilibria, 1989. **52**: p. 31-38.
37. Paricaud, P., A. Galindo, and G. Jackson, *Recent advances in the use of the SAFT approach in describing electrolytes, interfaces, liquid crystals and polymers.* Fluid Phase Equilibria, 2002. **194-197**: p. 87-96.
38. Chapman, W.G., et al., *Phase behavior applications of SAFT based equations of state--from associating fluids to polydisperse, polar copolymers.* Fluid Phase Equilibria, 2004. **217**(2): p. 137-143.
39. Andersen, S.I. and J.G. Speight, *Thermodynamic models for asphaltene solubility and precipitation.* Journal of Petroleum Science and Engineering, 1999. **22**(1-3): p. 53-66.
40. Johansson, B., et al., *Solubility and interaction parameters as references for solution properties II: Precipitation and aggregation of asphaltene in organic solvents.* Advances in Colloid and Interface Science. **147-148**: p. 132-143.
41. Mansoori, G.A., *Statistical Mechanical Models Of Asphaltene Flocculation And Collapse From Petroleum Systems*, in *Technical Meeting / Petroleum Conference Of The South Saskatchewan Section*. 1999, Petroleum Society of Canada: Regina.

42. Soulgani, B.S., et al., *A New Thermodynamic Scale Equation for Modelling of Asphaltene Precipitation Form Live Oil*, in *Canadian International Petroleum Conference*. 2009, Petroleum Society of Canada: Calgary, Alberta.
43. Sarma, H.K., *Can We Ignore Asphaltene in a Gas Injection Project for Light-Oils?*, in *SPE International Improved Oil Recovery Conference in Asia Pacific*. 2003, Society of Petroleum Engineers: Kuala Lumpur, Malaysia.

APPENDIX A: Recombined Oil Composition by CO_2

Vafaei Sefti et al

2.4942 mol% CO_2 injected

Components	Mol% liquid	Molecular weight(g/mol)	density(g/cm3)
N2	0.246	28.014	
CO2	4.039	44.01	
C1	24.381	16.04	
C2	3.185	30.07	
C3	4.17	44.097	
i-C4	0.636	58.124	
n-C4	1.479	58.124	
i-C5	0.841	72.151	
n-C5	0.951	72.151	
C6	1.896	86.178	0.664
PS1	22.029	142	0.868
PS2	16.973	274	0.873
PS3	4.481	350	0.877
Resin	10.843	603	1
Asphaltene	3.849	850	1.28

11.5012 mol% CO_2 injected

Components	Mol% liquid	Molecular weight(g/mol)	density(g/cm3)
N2	0.208	28.014	
CO2	10.146	44.01	
C1	21.372	16.04	
C2	2.898	30.07	
C3	3.866	44.097	
i-C4	0.595	58.124	
n-C4	1.39	58.124	
i-C5	0.796	72.151	
n-C5	0.902	72.151	
C6	1.806	86.178	0.664
PS1	21.198	142	0.868
PS2	16.351	274	0.873
PS3	4.317	350	0.877
Resin	10.446	603	1
Asphaltene	3.708	850	1.28

18.9838 mol% CO_2 injected

Components	Mol% liquid	Molecular weight(g/mol)	density(g/cm3)
N2	0.184	28.014	
CO2	14.271	44.01	
C1	19.312	16.04	
C2	2.693	30.07	
C3	3.647	44.097	
i-C4	0.565	58.124	
n-C4	1.327	58.124	
i-C5	0.763	72.151	
n-C5	0.867	72.151	
C6	1.745	86.178	0.664
PS1	20.656	142	0.868
PS2	15.951	274	0.873
PS3	4.211	350	0.877
Resin	10.191	603	1
Asphaltene	3.618	850	1.28

25.2194 mol% CO_2 injected

Components	Mol% liquid	Molecular weight(g/mol)	density(g/cm3)
N2	0.167	28.014	
CO2	17.177	44.01	
C1	17.847	16.04	
C2	2.542	30.07	
C3	3.484	44.097	
i-C4	0.543	58.124	
n-C4	1.279	58.124	
i-C5	0.74	72.151	
n-C5	0.841	72.151	
C6	1.7	86.178	0.664
PS1	20.285	142	0.868
PS2	15.68	274	0.873
PS3	4.14	350	0.877
Resin	10.019	603	1
Asphaltene	3.556	850	1.28

30.485 mol% CO_2 injected

Components	Mol% liquid	Molecular weight(g/mol)	density(g/cm3)
N2	0.155	28.014	
CO2	19.31	44.01	
C1	16.764	16.04	
C2	2.427	30.07	
C3	3.36	44.097	
i-C4	0.526	58.124	
n-C4	1.243	58.124	
i-C5	0.722	72.151	
n-C5	0.822	72.151	
C6	1.666	86.178	0.664
PS1	20.019	142	0.868
PS2	15.488	274	0.873
PS3	4.089	350	0.877
Resin	9.897	603	1
Asphaltene	3.513	850	1.28

35.0577 mol% CO_2 injected

Components	Mol% liquid	Molecular weight(g/mol)	density(g/cm3)
N2	0.145	28.014	
CO2	20.976	44.01	
C1	15.914	16.04	
C2	2.335	30.07	
C3	3.258	44.097	
i-C4	0.513	58.124	
n-C4	1.214	58.124	
i-C5	0.707	72.151	
n-C5	0.806	72.151	
C6	1.639	86.178	0.664
PS1	19.815	142	0.868
PS2	15.343	274	0.873
PS3	4.051	350	0.877
Resin	9.804	603	1
Asphaltene	3.48	850	1.28

40.0462 mol% CO_2 injected

Components	Mol% liquid	Molecular weight(g/mol)	density(g/cm3)
N2	0.136	28.014	
CO2	22.619	44.01	
C1	15.072	16.04	
C2	2.241	30.07	
C3	3.155	44.097	
i-C4	0.498	58.124	
n-C4	1.184	58.124	
i-C5	0.692	72.151	
n-C5	0.79	72.151	
C6	1.611	86.178	0.664
PS1	19.617	142	0.868
PS2	15.204	274	0.873
PS3	4.015	350	0.877
Resin	9.716	603	1
Asphaltene	3.449	850	1.28

42.5404 mol% CO_2 injected

Components	Mol% liquid	Molecular weight(g/mol)	density(g/cm3)
N2	0.132	28.014	
CO2	23.391	44.01	
C1	14.674	16.04	
C2	2.197	30.07	
C3	3.105	44.097	
i-C4	0.492	58.124	
n-C4	1.169	58.124	
i-C5	0.685	72.151	
n-C5	0.782	72.151	
C6	1.598	86.178	0.664
PS1	19.526	142	0.868
PS2	15.141	274	0.873
PS3	3.998	350	0.877
Resin	9.676	603	1
Asphaltene	3.435	850	1.28

46.0046 mol% CO_2 injected

Components	Mol% liquid	Molecular weight(g/mol)	density(g/cm3)
N2	0.126	28.014	
CO2	24.385	44.01	
C1	14.162	16.04	
C2	2.138	30.07	
C3	3.039	44.097	
i-C4	0.483	58.124	
n-C4	1.15	58.124	
i-C5	0.675	72.151	
n-C5	0.772	72.151	
C6	1.58	86.178	0.664
PS1	19.409	142	0.868
PS2	15.061	274	0.873
PS3	3.977	350	0.877
Resin	9.625	603	1
Asphaltene	3.417	850	1.28

48.77 mol% CO_2 injected

Components	Mol% liquid	Molecular weight(g/mol)	density(g/cm3)
N2	0.122	28.014	
CO2	25.136	44.01	
C1	13.774	16.04	
C2	2.094	30.07	
C3	2.988	44.097	
i-C4	0.476	58.124	
n-C4	1.135	58.124	
i-C5	0.668	72.151	
n-C5	0.764	72.151	
C6	1.567	86.178	0.664
PS1	19.322	142	0.868
PS2	15.002	274	0.873
PS3	3.962	350	0.877
Resin	9.588	603	1
Asphaltene	3.404	850	1.28

Hu et al

51.6 mol% CO_2 injected

Components	Mol% liquid	Molecular weight(g/mol)	density(g/cm3)
N2	0.439	28.014	
CO2	32.251	44.01	
C1	13.925	16.04	
C2	0.498	30.07	
C3	2.219	44.097	
i-C4	0.442	58.124	
n-C4	1.879	58.124	
i-C5	0.365	72.151	
n-C5	0.746	72.151	
C6	0.496	84.73	0.664
C7	0.414	91.26	0.738
C8	1.329	104.27	0.765
C9	1.645	118.97	0.781
C10	0.588	175	0.792
C11+	37.951	442	0.9215
Resin	3.507	850	1
Asphaltene	1.305	1000	1.28

63.8 mol% CO_2 injected

Components	Mol% liquid	Molecular weight(g/mol)	density(g/cm3)
N2	0.356	28.014	
CO2	35.875	44.01	
C1	12.174	16.04	
C2	0.458	30.07	
C3	2.083	44.097	
i-C4	0.418	58.124	
n-C4	1.786	58.124	
i-C5	0.349	72.151	
n-C5	0.714	72.151	
C6	0.477	84.73	0.664
C7	0.399	91.26	0.738
C8	1.285	104.27	0.765
C9	1.592	118.97	0.781
C10	0.569	175	0.792
C11+	36.798	442	0.9215
Resin	3.401	850	1
Asphaltene	1.266	1000	1.28

71.6 mol% CO_2 injected

Components	Mol% liquid	Molecular weight(g/mol)	density(g/cm3)
N2	0.316	28.014	
CO2	37.744	44.01	
C1	11.239	16.04	
C2	0.436	30.07	
C3	2.006	44.097	
i-C4	0.404	58.124	
n-C4	1.733	58.124	
i-C5	0.34	72.151	
n-C5	0.697	72.151	
C6	0.466	84.73	0.664
C7	0.392	91.26	0.738
C8	1.262	104.27	0.765
C9	1.565	118.97	0.781
C10	0.56	175	0.792
C11+	36.244	442	0.9215
Resin	3.35	850	1
Asphaltene	1.247	1000	1.28

80.2 mol% CO_2 injected

Components	Mol% liquid	Molecular weight(g/mol)	density(g/cm3)
N2	0.28	28.014	
CO2	39.463	44.01	
C1	10.358	16.04	
C2	0.414	30.07	
C3	1.929	44.097	
i-C4	0.391	58.124	
n-C4	1.681	58.124	
i-C5	0.331	72.151	
n-C5	0.68	72.151	
C6	0.456	84.73	0.664
C7	0.385	91.26	0.738
C8	1.242	104.27	0.765
C9	1.541	118.97	0.781
C10	0.552	175	0.792
C11+	35.763	442	0.9215
Resin	3.305	850	1
Asphaltene	1.23	1000	1.28

APPENDIX B: Legends Information in Flowcharts

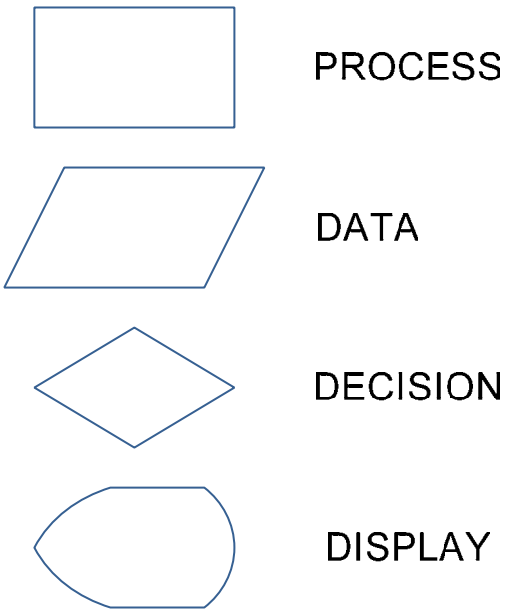

APPENDIX C: Compositional Simulation Command

```
RUNSPEC
============================================================

TITLE
  Asphaltene PRECIPITATION for CO2 Flooding

START
  1 JAN 2000  /

FIELD

GAS
OIL
WATER

DIMENS
 15 1 1  /

COMPS
8 /

EQLDIMS
1 200 /

TABDIMS
1 1 2* 2     /

--AIM
FULLIMP

--NOSIM

UNIFIN
UNIFOUT
```

```
NOECHO

-- Switch on Asphaltene deposition model

ASPHALTE
 WEIGHT  PORO  TAB /

GRID
============================================================

--Basic grid block sizes

BOX
 1  15   1   1   1   1  /

DX
  3*50 9*800 3*50
/

EQUALS
DY 1000   /
DZ   50   /
PORO  0.1 /
PERMX 500 /
PERMY 500 /
PERMZ 300 /
TOPS 4000 4* 1 1 /
/

-- Increase PV to provide pressure buffer and keep pres > psat

EQUALS
 MULTPV 2  /
/
```

```
-- Remove cells from "sump" of model

-- EQUALS
-- -- array  value  I1 I2  J1 J2  K1 K2
--   ACTNUM    0     2 10   1  1   2  3  /
-- /



--Properties section--------------------------------------------

PROPS

--Water saturation functions

SWFN
0.16  0      3
0.18  0      2
0.20  0.002  1
0.44  0.090  0.5
0.68  0.330  0.1
0.8   0.540  0.05
1.00  1.000  0.0 /

--Gas saturation functions

SGFN
0.00  0.000  0.0
0.04  0.005  0.0
0.12  0.026  0.0
0.24  0.078  0.0
0.36  0.156  0.0
0.48  0.260  0.0
0.60  0.400  0.0
0.72  0.562  0.0
0.84  0.800  0.0
/
```

```
--Oil saturation functions

SOF3
0.00  0.000  0.000
0.24  0.000  0.000
0.28  0.005  0.005
0.32  0.012  0.012
0.44  0.060  0.060
0.56  0.150  0.150
0.72  0.400  0.400
0.84  0.800  0.800 /

--Rock properties

ROCK
-- pres    cw
  3550  3.5E-6 /


-- Water properties

PVTW
-- pres    bw    cw     vw
  3500  1.03  3.0E-6  0.23 /


-- Standard conditions

STCOND
--Temp   Pressure
 60     14.7 /

-- Reservoir temperature (deg F)

RTEMP
```

```
 122 /


-- Equation of State

EOS
   PR  /

-- Modified Peng-Robinson EoS

PRCORR

-- Component names

CNAMES
      'CO2'   'C1'    'C3'    'C6'    'C10'   'C15'   'C20'    'ASPH'   /

-- Reservoir EoS properties

-- ... molecular weights

MW
      44.01  16.04    44.10    86.18    149.29    206.00    282.00    282.0   /

-- ... critical temperatures (R)

TCRIT
      547.56  343.00   665.70   913.40   1111.80   1270.00   1380.00  1380.00   /

-- ... critical pressures (psia)

PCRIT
      1069.8673 667.80   616.30   436.90    304.00    200.00    162.00   162.00   /

-- ... critical Z-factors
```

```
ZCRIT
      0.27414  0.290    0.277    0.264    0.257    0.245    0.235    0.235   /

--  ... accentric factors

ACF
      0.225   0.013    0.153    0.301    0.489    0.650    0.850    0.850   /

-- ... binary interaction coefficients

BIC
       0.01
       0.01      0
       0.01      0       0
       0.01      0       0       0
       0.05   0.005      0       0       0
       0.05   0.005      0       0       0       0
       0.05   0.005      0.005   0.005   0.005   0.005   0.005   /

-- Specify initial liquid composition

ZI
  0    0.50    0.03    0.07     0.20     0.10    0.08    0.02   /


-- Asphaltene parameters

-- ... asphaltene floc components

ASPFLOC
-- first  last  floc
    7     7     8  /

-- ... define asphaltene concentration limits

--ASPP1P
```

```
-- 'P' /
--ASPREWG
--  pres   %_wt
--  1000.0   15.0
--  2000.0    5.0
--  3900.0   35.0
--  4200.0   70.0
--  8000.0  100.0  /

-- ASPP1P
--  'C' 1 /
-- ASPREWG
-- -- conc   %_wt
--    0.000   100.0
--    0.010    90.0
--    0.080    20.0
--    0.150    10.0
--    1.000     0.0
--   10.000     0.0  /

ASPP1P
'P' /

ASPREWG
-- taken from asphaltene model - ADE
--  pres   %_wt
 1500.0   15.0
 2500.0    5.0
 4000.0   35.0
 4200.0   70.0
 8000.0  100.0  /



-- ... ashphaltene floc rates
-- (set here to cause faster floc degradation than formation)
```

```
ASPFLRT
-- CMP6
   0.010
   0.0001  /

-- ... asphaltene deposition

ASPDEPO
-- adsorp   plug  entrain   Vcr
  5.0E-3    0.0   1.0E-7   2500  /

-- ... asphaltene damage ratio

ASPKDAM
-- exp
3.
/
SKIP
-- deposit   mult
    0.0     1.0
    1.0E-5  0.99
    1.0E-4  0.90
    1.0E-3  0.80
    1.0E-2  0.50  /
ENDSKIP

-- ... asphaltene viscosity change
ASPVISO
-- vfrac    mult
   0.0     1.0
   0.01    1.2
   0.1     1.5
   1.0    10.0  /

SOLUTION
============================================================
```

```
EQUIL
-- zdat  pdat  owc  pcow   goc  pcog  dummy  dummy  Ninit
  4000  4000 4060    0  2000    0    1      1   1*   /

RPTRST
 PRESSURE SOIL SGAS SWAT XMF YMF RPORV
 ASPADS ASPDOT ASPEN ASPFL ASPKDM ASPLU ASPREW ASPVOM ASPLIM ASPFRD  /


SUMMARY
============================================================


FGOR
FWCT
FOPR
FOPT
FGIR
FGIT
FWIR
FWIT
FVPR
FVIR
FPR
FOSAT
FGSAT
FLPR
FLPT

WBHP
 PROD  WINJ  /

TCPU
ELAPSED
NEWTON
```

BMLSC

-- block component

1 1 1 7 /

2 1 1 7 /

3 1 1 7 /

4 1 1 7 /

5 1 1 7 /

6 1 1 7 /

7 1 1 7 /

8 1 1 7 /

9 1 1 7 /

10 1 1 7 /

11 1 1 7 /

12 1 1 7 /

13 1 1 7 /

14 1 1 7 /

15 1 1 7 /

/

BMLSC

-- block component

1 1 1 8 /

2 1 1 8 /

3 1 1 8 /

4 1 1 8 /

5 1 1 8 /

6 1 1 8 /

7 1 1 8 /

8 1 1 8 /

9 1 1 8 /

10 1 1 8 /

11 1 1 8 /

12 1 1 8 /

13 1 1 8 /

14 1 1 8 /

15 1 1 8 /

/

BMLSC

-- block component

1 1 1 1 /

2 1 1 1 /

3 1 1 1 /

4 1 1 1 /

5 1 1 1 /

6 1 1 1 /

7 1 1 1 /

8 1 1 1 /

9 1 1 1 /

10 1 1 1 /

11 1 1 1 /

12 1 1 1 /

13 1 1 1 /

14 1 1 1 /

15 1 1 1 /

/

BMLSC

-- block component

1 1 1 2 /

2 1 1 2 /

3 1 1 2 /

4 1 1 2 /

5 1 1 2 /

6 1 1 2 /

7 1 1 2 /

8 1 1 2 /

9 1 1 2 /

10 1 1 2 /

11 1 1 2 /

12 1 1 2 /

13 1 1 2 /

14 1 1 2 /

```
 15  1  1  2 /
/

BMLSC
-- block component
  1  1  1  3 /
  2  1  1  3 /
  3  1  1  3 /
  4  1  1  3 /
  5  1  1  3 /
  6  1  1  3 /
  7  1  1  3 /
  8  1  1  3 /
  9  1  1  3 /
 10  1  1  3 /
 11  1  1  3 /
 12  1  1  3 /
 13  1  1  3 /
 14  1  1  3 /
 15  1  1  3 /
/

BMLSC
-- block component
  1  1  1  4 /
  2  1  1  4 /
  3  1  1  4 /
  4  1  1  4 /
  5  1  1  4 /
  6  1  1  4 /
  7  1  1  4 /
  8  1  1  4 /
  9  1  1  4 /
 10  1  1  4 /
 11  1  1  4 /
 12  1  1  4 /
```

13 1 1 4 /

14 1 1 4 /

15 1 1 4 /

/

BMLSC

-- block component

1 1 1 5 /

2 1 1 5 /

3 1 1 5 /

4 1 1 5 /

5 1 1 5 /

6 1 1 5 /

7 1 1 5 /

8 1 1 5 /

9 1 1 5 /

10 1 1 5 /

11 1 1 5 /

12 1 1 5 /

13 1 1 5 /

14 1 1 5 /

15 1 1 5 /

/

BMLSC

-- block component

1 1 1 6 /

2 1 1 6 /

3 1 1 6 /

4 1 1 6 /

5 1 1 6 /

6 1 1 6 /

7 1 1 6 /

8 1 1 6 /

9 1 1 6 /

10 1 1 6 /

11 1 1 6 /

```
 12  1  1  6 /
 13  1  1  6 /
 14  1  1  6 /
 15  1  1  6 /
/

BMLSC
-- block component
  1  1  1  7 /
  2  1  1  7 /
  3  1  1  7 /
  4  1  1  7 /
  5  1  1  7 /
  6  1  1  7 /
  7  1  1  7 /
  8  1  1  7 /
  9  1  1  7 /
 10  1  1  7 /
 11  1  1  7 /
 12  1  1  7 /
 13  1  1  7 /
 14  1  1  7 /
 15  1  1  7 /
/

-- Asphaltene grid block parameters

BASPADS
  1  1  1  /
  2  1  1  /
  3  1  1  /
  4  1  1  /
  5  1  1  /
  6  1  1  /
  7  1  1  /
  8  1  1  /
```

9 1 1 /

10 1 1 /

11 1 1 /

12 1 1 /

13 1 1 /

14 1 1 /

15 1 1 /

/

BASPLUG

1 1 1 /

2 1 1 /

3 1 1 /

4 1 1 /

5 1 1 /

6 1 1 /

7 1 1 /

8 1 1 /

9 1 1 /

10 1 1 /

11 1 1 /

12 1 1 /

13 1 1 /

14 1 1 /

15 1 1 /

/

BASPENT

1 1 1 /

2 1 1 /

3 1 1 /

4 1 1 /

5 1 1 /

6 1 1 /

7 1 1 /

8 1 1 /

9 1 1 /

10 1 1 /

11 1 1 /

12 1 1 /

13 1 1 /

14 1 1 /

15 1 1 /

/

BASPDOT

1 1 1 /

2 1 1 /

3 1 1 /

4 1 1 /

5 1 1 /

6 1 1 /

7 1 1 /

8 1 1 /

9 1 1 /

10 1 1 /

11 1 1 /

12 1 1 /

13 1 1 /

14 1 1 /

15 1 1 /

/

BASPREW

1 1 1 /

2 1 1 /

3 1 1 /

4 1 1 /

5 1 1 /

6 1 1 /

7 1 1 /

8 1 1 /

9 1 1 /

10 1 1 /

11 1 1 /

12 1 1 /

13 1 1 /

14 1 1 /

15 1 1 /

/

BASPRET

1 1 1 /

2 1 1 /

3 1 1 /

4 1 1 /

5 1 1 /

6 1 1 /

7 1 1 /

8 1 1 /

9 1 1 /

10 1 1 /

11 1 1 /

12 1 1 /

13 1 1 /

14 1 1 /

15 1 1 /

/

BASPLIM

1 1 1 /

2 1 1 /

3 1 1 /

4 1 1 /

5 1 1 /

6 1 1 /

7 1 1 /

8 1 1 /

9 1 1 /

10 1 1 /

11 1 1 /

12 1 1 /

13 1 1 /

14 1 1 /

15 1 1 /

/

BASPFRD

1 1 1 /

2 1 1 /

3 1 1 /

4 1 1 /

5 1 1 /

6 1 1 /

7 1 1 /

8 1 1 /

9 1 1 /

10 1 1 /

11 1 1 /

12 1 1 /

13 1 1 /

14 1 1 /

15 1 1 /

/

BASPKDM

1 1 1 /

2 1 1 /

3 1 1 /

4 1 1 /

5 1 1 /

6 1 1 /

7 1 1 /

8 1 1 /

9 1 1 /

10 1 1 /

11 1 1 /

12 1 1 /

13 1 1 /

14 1 1 /

15 1 1 /

/

BASPVOM

1 1 1 /

2 1 1 /

3 1 1 /

4 1 1 /

5 1 1 /

6 1 1 /

7 1 1 /

8 1 1 /

9 1 1 /

10 1 1 /

11 1 1 /

12 1 1 /

13 1 1 /

14 1 1 /

15 1 1 /

/

BASPFL

1 1 1 7 /

2 1 1 7 /

3 1 1 7 /

```
 4  1  1  7 /
 5  1  1  7 /
 6  1  1  7 /
 7  1  1  7 /
 8  1  1  7 /
 9  1  1  7 /
10  1  1  7 /
11  1  1  7 /
12  1  1  7 /
13  1  1  7 /
14  1  1  7 /
15  1  1  7 /
 1  1  1  8 /
 2  1  1  8 /
 3  1  1  8 /
 4  1  1  8 /
 5  1  1  8 /
 6  1  1  8 /
 7  1  1  8 /
 8  1  1  8 /
 9  1  1  8 /
10  1  1  8 /
11  1  1  8 /
12  1  1  8 /
13  1  1  8 /
14  1  1  8 /
15  1  1  8 /
/


-- Other block parameters

BXMF
 1  1  1  7 /
 2  1  1  7 /
 3  1  1  7 /
```

4 1 1 7 /

5 1 1 7 /

6 1 1 7 /

7 1 1 7 /

8 1 1 7 /

9 1 1 7 /

10 1 1 7 /

11 1 1 7 /

12 1 1 7 /

13 1 1 7 /

14 1 1 7 /

15 1 1 7 /

1 1 1 8 /

2 1 1 8 /

3 1 1 8 /

4 1 1 8 /

5 1 1 8 /

6 1 1 8 /

7 1 1 8 /

8 1 1 8 /

9 1 1 8 /

10 1 1 8 /

11 1 1 8 /

12 1 1 8 /

13 1 1 8 /

14 1 1 8 /

15 1 1 8 /

/

BPR

1 1 1 /

2 1 1 /

3 1 1 /

4 1 1 /

5 1 1 /

6 1 1 /

7 1 1 /

8 1 1 /

9 1 1 /

10 1 1 /

11 1 1 /

12 1 1 /

13 1 1 /

14 1 1 /

15 1 1 /

/

BDENO

1 1 1 /

2 1 1 /

3 1 1 /

4 1 1 /

5 1 1 /

6 1 1 /

7 1 1 /

8 1 1 /

9 1 1 /

10 1 1 /

11 1 1 /

12 1 1 /

13 1 1 /

14 1 1 /

15 1 1 /

/

BPORV

1 1 1 /

2 1 1 /

3 1 1 /

```
 4  1  1  /
 5  1  1  /
 6  1  1  /
 7  1  1  /
 8  1  1  /
 9  1  1  /
10  1  1  /
11  1  1  /
12  1  1  /
13  1  1  /
14  1  1  /
15  1  1  /
/
```

BOVIS

```
 1  1  1  /
 2  1  1  /
 3  1  1  /
 4  1  1  /
 5  1  1  /
 6  1  1  /
 7  1  1  /
 8  1  1  /
 9  1  1  /
10  1  1  /
11  1  1  /
12  1  1  /
13  1  1  /
14  1  1  /
15  1  1  /
/
```

RUNSUM

```
SCHEDULE
============================================================

--Define injection and production wells

WELSPECS
-- Well   Group  I0 J0  depth  phase
  WATINJ  FIELD   1  1   1*  WAT  /
  PROD    FIELD  15  1   1*  OIL  /
/

COMPDAT
-- Well    I  J  K1  K2  Status
  WATINJ   1  1   1   1   OPEN   /
  PROD    15  1   1   1   OPEN   /
/

WCONPROD
-- Well  Status  Mode  Orat Wrat  Grat  Lrat   Resv   BHP
  PROD   OPEN   RESV  1*   1*    1*    1*    3500   500  /
/

WCONINJE
-- Well  Type  Status  Mode  Surf  Resv   BHP
  WATINJ WAT   OPEN   RESV   1*  25000  4400  /
/

-- Increase PI to avoid premature switch to BHP control

-- WPIMULT
-- -- Well  Value
--    WINJ  100.0  /
-- /

-- Composition of injected fluid (native oil)
```

```
WELLSTRE
-- name    CO2   C1    C3    C6    C10    C15    C20   ASPH
--   IOIL   0.50   0.03   0.07   0.20   0.15   0.05   0.00   /
  CO2   1   0   0   0   0   0   0   0 /
/

-- Link well to type of injected fluid

WINJGAS
-- Well    Type  Stream
  WATINJ  STRE   CO2  /
/



TUNING
1* 1* 1e-05 1e-03 1.2 5* /
 /
 /

-- Reporting frequency

--RPTRST
--  PRESSURE SOIL SGAS SWAT XMF YMF RPORV
--  ASPADS ASPRET ASPLU ASPENT ASPDOT ASPFL ASPKDM ASPREW ASPVOM ASPLIM ASPFRD /

RPTPRINT
 1 4*0 1 /

-- Simulate depletion and re-pressurisation periods

TSTEP
 20*50  /

-- Switch off producer and start injecting to re-pressurise

-- WELOPEN
```

```
-- -- Well  Status
--    WINJ   OPEN  /
--    PROD   SHUT  /
-- /

TSTEP
  20*10  /

-- Switch off injector and watch change in asphaltenes

-- WELOPEN
-- -- Well  Status
--    WINJ   SHUT  /
-- /

TUNING
1* 1* 1e-05 1e-03 1.2 5* /
 /
 /

TSTEP
 18*100  /
/

TSTEP
 0.01 /

RPTPRINT
 1 0 0 0 0 1  /

-- Write out restart record

SAVE
/

-- Reduce the pressure once more ....
```

```
-- WELOPEN
-- -- name  status
--    PROD    OPEN  /
-- /

NEXTSTEP
 0.01  /

TUNING
1* 1* 1e-05 1e-03 1.2 5* /
 /
 /

TSTEP
 20*50  /

RPTPRINT
 1 1 0 0 0 1  /

TSTEP
 0.01 /

RPTPRINT
 1 0 0 0 0 1  /

-- Watch for deposition by plugging

-- WELTARG
-- -- name   mode  target
--    PROD   RESV   2500  /
--    WINJ   RESV   2550  /
-- /

-- WELOPEN
-- -- name  status
```

```
--   PROD   OPEN  /
--   WINJ   OPEN  /
-- /

NEXTSTEP
 0.01  /

TUNING
1* 1* 1e-05 1e-03 1.2 5* /
 /
 /

TSTEP
 20*50  /

RPTPRINT
 1 1 0 0 0 1  /

TSTEP
 0.01 /

RPTPRINT
 1 0 0 0 0 1  /

-- Increase rate to induce entrainment

-- WELTARG
-- -- name   mode  target
--   PROD   RESV   5000  /
--   WINJ   RESV   5100  /
/

NEXTSTEP
 0.01  /

TUNING
```

```
1* 1* 1e-05 1e-03 1.2 5* /
 /
 /

TSTEP
  20*50  /

RPTPRINT
  1 1 0 0 0 1  /

TSTEP
  0.01 /

END
```